POLISH
ACADEMY
OF SCIENCES

COMMITTEE
OF MACHINE
ENGINEERING

SCIENTIFIC PROBLEMS OF MACHINES OPERATION AND MAINTENANCE

ZAGADNIENIA EKSPLOATACJI MASZYN

TRIBOLOGY • RELIABILITY • TEROTECHNOLOGY
DIAGNOSTICS • SAFETY • ECO-ENGINEERING

TRIBOLOGIA • NIEZAWODNOŚĆ • EKSPLOATYKA
DIAGNOSTYKA • BEZPIECZEŃSTWO • EKOINŻYNIERIA

3 (159)
Vol. 44
2009

Institute for Sustainable Technologies – National Research Institute, Radom

Mailing address: Scientific Problems of Machines Operation and Maintenance
Institute for Sustainable Technologies – National Research Institute
ul. Pułaskiego 6/10, 26-600 Radom, Poland
Phone (48-48) 364 47 90
E-mail: ewa.szczepanik@itee.radom.pl

The figures have been directly reproduced from the originals submitted by the Authors.

Publishing House of Institute for Sustainable Technologies – National Research Institute
26-600 Radom, K. Pułaskiego 6/10 St., phone (48-48) 364-42-41, fax (048) 364-47-65
www.tribologia.org
2078

SCIENTIFIC PROBLEMS
OF MACHINES OPERATION
AND MAINTENANCE
3 (159) 2009

CONTENTS

SPIS TREŚCI

SCIENTIFIC PROBLEMS
OF MACHINES OPERATION
AND MAINTENANCE
3 (159) 2009

BEZJAZYCHNYJ VYACHESLAV FEOKTISTOVICH*,
FOMENKO ROMAN NIKOLAEVICH*

The influence of tribological characteristics of coated tools on cutting process and the parameters of surface layer

Key words

The parameters of surface layer, coating, turning, tool, optimal cutting speed.

Słowa kluczowe

Parametry warstwy wierzchniej, powłoka, toczenie, narzędzie, prędkość skrawania.

Summary

The influence of wear-resistant coatings having different friction coefficients on a cutting force, chip thickening coefficient, coefficient of chip friction on the face of a tool and temperature in the cutting zone have been researched.

1. Introduction

The most important production properties are reliability and endurance. These properties provide product safety and competitiveness. The main cause leading to breakdown of parts is fatigue cracks. Such cracks appear and propagate in thin surface layers of parts. In order to hamper crack growth, the

* Rybinsk State Academy of Aviation Technology named after P.A. Solovjev, 152934, Rybinsk, Yaroslavl region, St. Pushkin, 53; Russia, Phone Office: (4855) 222091, Fax: (4855) 213964 E-mail: fomenko85@mail.ru

surface layer has to exhibit certain features. They are roughness, residual stress, and strain hardening, which depend on the characteristics of the cutting operation.

The cutting force, temperature of cutting, the depth of wear hardening, and the degree of deformation are referring to as the main characteristics of a cutting operation. These characteristics influence on the parts' quality, reliability, and endurance. Technological conditions of cutting, such as tools geometry, processing conditions, work material properties and tooling material properties, including tribological feathers, determine the characteristics of the cutting process. Therefore, there is a need to select optimal cutting conditions to provide the required part quality. In order to select optimal cutting conditions, there is the necessity to have a special method, which takes into consideration the relationship between parts quality and technological conditions.

2. Theoretical parts

At the Rybinsk State of Aviation Technology academy named after P.A. Solovjev (Russia) there was developed the method, which permits one to estimate the optimal cutting conditions. On the base of this method, underlay a functional connection between cutting rate, tools geometry and the parameters of surface layer, the accuracy of machining and the rigidity of manufacturing system, including work material and tool material properties.

But all advanced tools have wear-resistant coatings that exhibit specific properties. Wear-resistant coatings have a low friction coefficient in the consequence of weak adhesion interaction between the covering material and the work material. They influence the cutting process and quality parameters of the surface layer. Tools coverings reduce chips contact length with tools surface, cutting force, the temperature of cutting, and the deformation of cut allowance. It is due to the increase of the chip flow angle.

In order to provide high part quality, one should calculate the "optimal cutting speed" v_O. Optimal cutting rates (v_O, S_O) correspond to optimal cutting temperature. It is constant in magnitude for the defined combination work – tool material [1]. When machining with this temperature, maximum tool life, minimal roughness of machined surface *Ra*, and minimal surface defects occur. Therefore, these cutting rates should be used when finishing work is performed for parts, which work in a corrosive medium and high temperature, because the surface layer has to contain minimal defects. For estimating the optimal cutting speed v, the equation is obtained by Silin S.S. [2]:

$$v_O = \frac{C_O \cdot a}{a_1}\left(\frac{a_1 \cdot b_1 \cdot c\rho \cdot \Theta}{Pz_{\min}}\right)^n \tag{1}$$

where a_1, b_1 – is the thickness and the width of cut respectively [m]; a – is the coefficient of the temperature conductivity of the work material [m^2/s]; cρ – is the specific heat capacity per unit volume [J/($m^3 \cdot s \cdot$ degree)]; Θ – is the temperature in the cutting area, °C; n, C_o – are coefficients, which depend on the properties of work material; Pz_{min} – is a minimal stabilised cutting force [N].

The series of experiments were performed in this work to reach the following purposes:

1. To investigate the influence of tribological characteristics of coated tools on cutting process and the parameters of surface layer; and,
2. To define optimal cutting speed for tools with different coatings.

3. Experimental conditions

The wide range of cutting rates, different work materials and coated tools were selected for performing experiments (Table 1).

In the capacity of tools, replaceable inserts 120412, material – VK6R (chemical composition: Co – 6%, basis – WC) and TT7K12 (chemical composition: Co – 12%, Ti – 1%, Ta – 1%, basis – WC) were used. The different composite nanolaminated ion-plasmous coatings were deposited on the replaceable inserts: (Ti;Si)N, (Ti,Si,Zr)CN and (Ti;Si;Al)N. The other group replaceable inserts was modified by implanting of nanoparticle TiB_2, Al_2O_3, Ta_2O_3 and ZrB_2 in the work surface of tools. All selected coatings have been characterised by the minimal adhesive of the tool surfaces with the work material, and they also have been provided maximum tool life [3].

Table 1. Experimental conditions

Changing parameters		Work material				
		Heat-resistant alloy (CrNi77TiAlW) EI437		Stainless steel (05Cr12Ni2Co3Mo2WV) EK26		Titaniu m alloy OT4
Tools geometry	Cutting angle, γ°	5		8		0
	Relief angle, α°	10		12		10
	Lead angle, φ, φ_1°	45				
	Nose radius, *r*, [mm]	1,2				
Cutting rate	Deph *t* [mm]	0.25; 0.5; 0.75; 1				
	Feed *S* [mm/rev]	0.07; 0.14; 0.2; 0.32				
	Speed *v* [m/min]	14-170		33-190		15-130
Tool material		VK6R	TT7K12	VK6R	TT7K12	VK6R
Coating		(Ti,Si)N	Ta_2O_3	(Ti,Si)N	Ta_2O_3	(Ti,Si)N
		(Ti,Si,Al)N	ZrB_2	(Ti,Si,Al) N	ZrB_2	(Ti,Si,Zr)CN
		TiB_2		TiB_2		ZrB_2
		Al_2O_3		Al_2O_3		Al_2O_3

The regular engine lathe NH 22 performed the machining. The cutting forces were measured using a universal tool dynamometer UDM – 600, which was connected with a analogue-digital converter and personal computer. The temperature was measured by means of a dynamic thermocouple of work material – tooling material.

4. Results and discussion

Figure 1 shows the friction coefficient, which was determined for different combinations of work materials – coated tools. As clearly shown, the uncoated tools' friction coefficient is larger then ones of coated tools. The main reason is that the tool coating decreases the adhesive interaction with a work material.

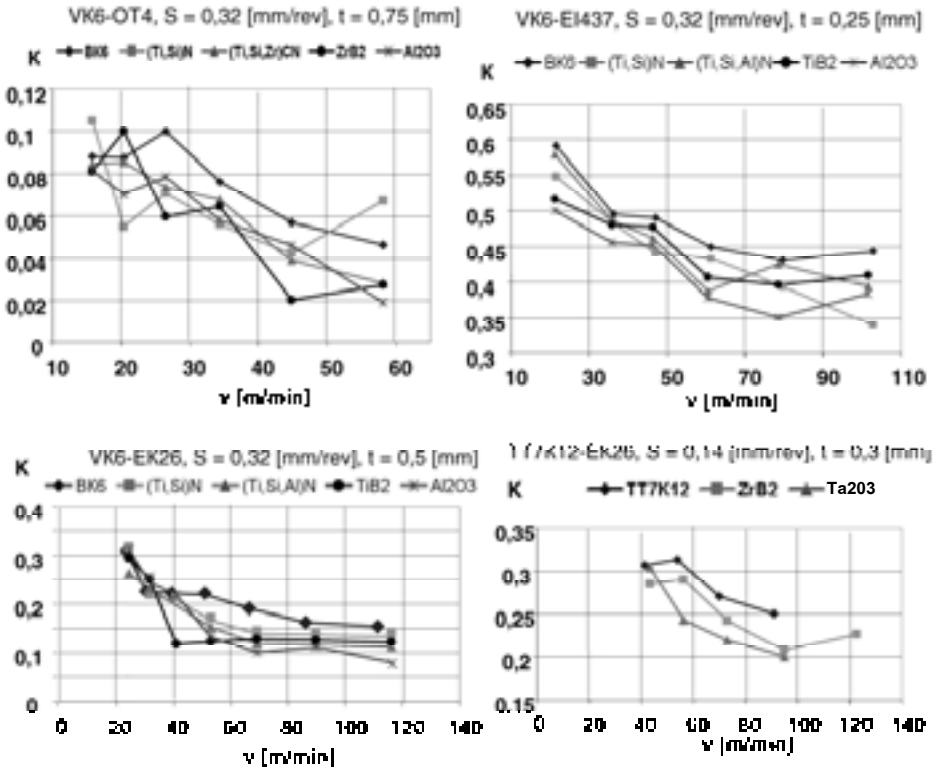

Fig. 1. Friction coefficient K against cutting speed *v* (symbols in table 1)

In order to adjust the estimate the influence of coated tools on the parameters of surface layer, one has to determine the influence of coated tools on criterion *B*. This criterion is one of the major parameters, which used for estimating of roughness, residual stress, and strain hardening in the part's surface layer.

$B = tg\beta_1$ – Is the quantity, which defines the degree of machining allowance for plastic deformation and the deformation of the part's surface layer, β_1 – is an angle of shear plane.

The quantity β_1 was estimated by means of Tim's I. A. formula using a chip reduction coefficient k_a. It was determined experimentally [2].

$$k_a = \frac{\cos(\beta_1 - \gamma)}{\sin\beta_1},$$

where γ – is a cutting angle.

Figure 2 shows the dependence of criterion *B* on technological conditions of operation.

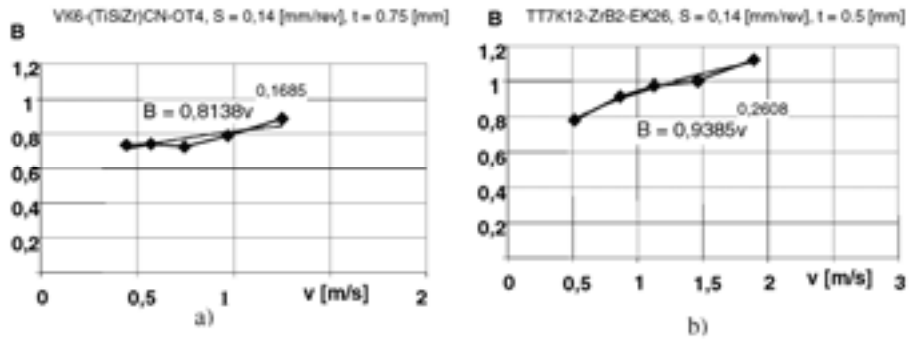

Fig. 2. Comparison the criterion B and technological conditions of operation: a) Work material – the titanium alloy OT4, tool – VK6R, coating – (Ti,Si,Zr)CN; b) Work material – the stainless steel EK26, tool – TT7K12, coating – ZrB_2

It is clearly shown that during increasing cutting speed *v* the criterion B increases too. It is the reason for increasing of an angle of shear plane β_1. The angle of shear plane β_1 increases, because the materials ultimate stress σ_B is reduced by reason of the increasing of rate of deformation and temperature in the cutting area.

The criterion B dependence on criterion Pe in the form of equation $B = C_1 \cdot Pe^{n_1}$ has been performed. The example of equation is illustrated by Figure 3.

In order to estimate optimal cutting speed v_O the dependencies of cutting force and temperature on cutting rate have been performed. Figure 4 shows that the optimal cutting temperature is $\theta_{OPT} = 840°C$.

$$Pe = \frac{v \cdot a_1}{a}$$

Criterion Pe defines the degree of influence of the cutting rate $v \cdot a_1$ as compared with the coefficient of the temperature conductivity of the work material *a*.

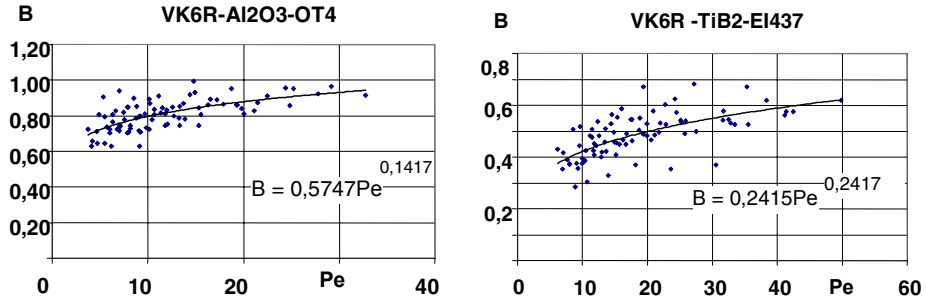

Fig. 3. Comparison the criterion B and Criterion Pe

Thus, using the equation in the form of $B = C_1 \cdot Pe^{n_1}$, one can estimate criterion B in a wide-range of cutting rate and tool shape.

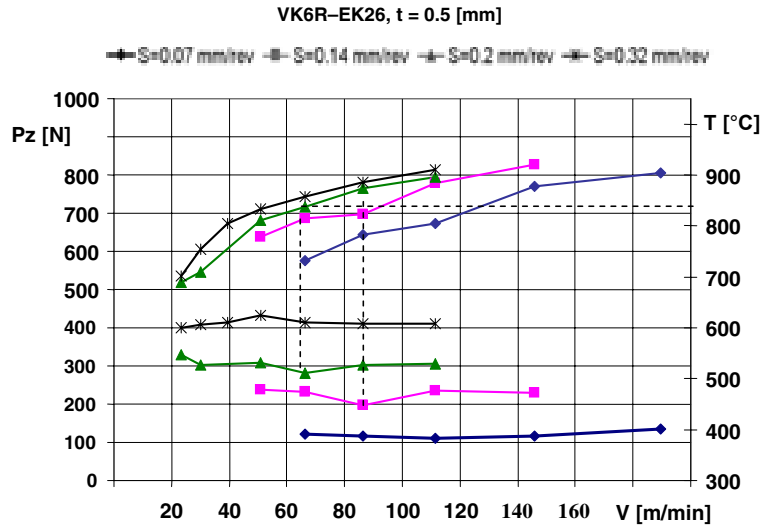

Fig. 4. Comparison the cutting force *Pz* and temperature of cutting *T* against cutting speed *v* and feet *S*, work material – stainless steel EK26, tool – VK6R

The criterion A dependence on criterion Pe in the form of equation $Pe = C_O \cdot A^n$ has been performed. The magnitude of coefficients C_O and *n* for some combination work material – coated tool are in Table 2.

$$A = \frac{S \cdot t \cdot c\rho \cdot \Theta}{Pz}$$

A – energy criterion, which defines the relationship of chip quantity of heat with general quantity of heat.

Table 2. Magnitude of coefficients C_O and n

Material	VK6R–EK26	VK6R–EK26–(Ti,Si)N	VK6R–EK26–Al_2O_3
Equation	$Pe = 13.16 \cdot A^{2.47}$	$Pe = 13.6 \cdot A^{2.48}$	$Pe = 13.53 \cdot A^{2.53}$

The examples of power dependencies for estimating of minimal cutting force Pz, which depend on cutting rate t and S, have been given in Table 3.

Table 3. Power dependence $Pz_{\min} = c_{Pz} \cdot t^{x_0} \cdot S^{x}$

Material	VK6R–EK26	VK6R–EK26–(Ti,Si)N	VK6R–EK26–Al_2O_3
Equation	$Pz = 1700 \cdot t^{0.77} \cdot S^{\frac{0.72}{t^{0.083}}}$	$Pz = 1598 \cdot t^{0.685} \cdot S^{\frac{0.7663}{t^{0.106}}}$	$Pz = 1269 \cdot t^{0.737} \cdot S^{\frac{0.695}{t^{0.044}}}$

Thus, on the base of obtained power dependencies, one can make a equation of machinability to estimate of optimal cutting speed v_O for different combination work material – coated tools. The equations of machinability for considered examples are given in Table 4.

Table 4. The equations of machinability

Materials	VK6R–EK26	VK6R–EK26–(Ti,Si)N	VK6R–EK26–Al_2O_3
Cutting rate	t = 0.5 [mm]; S = 0.32 [mm/rev]		
Equation	$v_O = \frac{2{,}31 \cdot a}{a_1}\left(\frac{a_1 \cdot b_1 \cdot c\rho}{t^{0,77} \cdot S^{\frac{0,72}{t^{0,083}}}}\right)$	$v_O = \frac{2{,}76 \cdot a}{a_1}\left(\frac{a_1 \cdot b_1 \cdot c\rho}{t^{0,68} \cdot S^{\frac{0,766}{t^{0,106}}}}\right)^{2,4}$	$v_O = \frac{4{,}76 \cdot a}{a_1}\left(\frac{a_1 \cdot b_1 \cdot c\rho}{t^{0,737} \cdot S^{\frac{0,695}{t^{0,044}}}}\right)^{2,5}$
Friction coefficient **K** (fig. 1) v=80[m/min]	0.17	0.14	0.1
$\boldsymbol{v_O}$ [m/min]	66.5	82.8	119.2

5. Conclusion

The optimal cutting speed of coated tool exceeds the optimal cutting speed of the uncoated tool. Therefore, the lower the coating friction coefficient, the higher the optimal cutting speed.

References

[1] Makarov A. D. The optimization of cutting operation. Moscow. 1976 p. 278
[2] Silin S. S. Similitude method of cutting. Moscow. 1979 p. 152
[3] Bruhov V. V. The increasing of tools lifetime after ion-implanting. Tomsk. 2003 p. 120

Manuscript received by Editorial Board, March 1st, 2010

Wpływ charakterystyk tribologicznych narzędzi z powłokami na proces skrawania i własności warstwy wierzchniej

S t r e s z c z e n i e

Przedstsawiono wyniki badań wpływu powłok przeciwzużyciowych, wykazujących zróżnicowane współczynniki tarcia na siłę skrawania, tarcie wióra na powierzchni narzędzia skrawajacego oraz temperaturę w strefie obróbki.

SCIENTIFIC PROBLEMS
OF MACHINES OPERATION
AND MAINTENANCE
3 (159) 2009

ALEKSANDAR VENCL*

Tribological properties of thixocasted and heat-treated hypoeutectic Al-Si alloy A356

Key words

Al-Si alloy, thixocasting, dry and lubricated sliding condition, wear, friction.

Słowa kluczowe

Stop Al-Si, tarcie suche, smarowanie, zużycie, tarcie.

Summary

This paper presents results of structural, mechanical and tribological tests of thixocasted and heat-treated hypoeutectic Al-Si alloy A356 (EN-Al Si7Mg0.3). The results of tribological tests were analysed and compared with the results of grey cast iron, which was chose as a standard material for cylinder blocks. The pin-on-disc tribometer was used to carry out tribological tests under dry and lubricated sliding conditions at different loads and speeds. The results showed that thixocasted and heat-treated Al-Si alloy under dry sliding conditions, for applied loads interval, could not be satisfactorily used since plastic flow of the material occurs. However, under lubricated sliding conditions tested material showed a low coefficient of friction without any plastic deformation.

* Tribology Laboratory, Mechanical Engineering Faculty, University of Belgrade, 11120 Belgrade 35, Serbia, avencl@mas.bg.ac.rs

1. Introduction

The use of light alloys in the transport industry is becoming a stringent need, because weight saving is one of the most important target in new vehicles design. Cast aluminium-silicon (Al-Si) alloys are widely used for the production of various automotive components, since silicon is one of a few alloying elements that does not increase the density of aluminium alloys. Aluminium alloys with moderate silicon levels, like A356, are typically used. Unfortunately, these alloys have their shortcomings that reflected, first of all, in inappropriate tribological properties of these materials. New production technologies, like thixocasting, are one of the possible solutions [1-4]. Additionally, the heat treatment to the T6 condition improves the wear resistance due to the higher material hardness [5].

As far as thixocasted Al-Si alloys are concerned, their improved mechanical properties over conventionally cast Al-Si alloys have been proven in many studies [6-8], while only a few studies dealing with tribological properties of thixocasted Al-Si alloys have been undertaken. Kang and Jung [4] showed that wear resistance of a thixoformed hypoeutectic Al-Si alloy could be very similar to cast iron if appropriate process parameters are used. Lasa and Rodriguez-Ibabe [9] also investigated two hypoeutectic Al-Si alloys produced with thihoforming and they found improvements of wear behaviour compared to the similar alloys cast in conventional metallic moulds. This was attributed to the fine, homogeneous, globular microstructure and the smaller spacing of the primary silicon particles in thihoformed alloys. Improvements of wear behaviour gained with additional heat treatment of thixocasted Al-Si alloys were explained with the improvements of their mechanical properties.

This paper presents the results of structural, mechanical and tribological tests of thixocasted and heat-treated hypoeutectic Al-Si alloy A356 (EN-Al Si7Mg0.3). The results of tribological tests, under dry and lubricated sliding conditions, were analysed and compared with the results of grey cast iron, which was chosen as a standard material for cylinder blocks.

2. Experimental procedure

2.1. Materials and heat treatments

Two sets of test specimens were used in this investigation. The first of test specimens was made of thixocasted and heat-treated hypoeutectic Al-Si alloy A356 (EN AlSi7Mg0.3), ref. as Thixo T6. According to the thixocasting procedure the A356 alloy was first obtained in the form of cylindrical billets, through magnetohydrodynamic (MHD) stirring and casting. MHD stirring involves electromagnetically stirring of the alloy in the semi-solid state, in order to break up the existing dendrites. After that, the billets were additionally heated

up (to app. 580°C), then placed in a high-pressure die casting press, and injected (at 210 MPa) directly into the die (preheated at 200 to 250°C). All thixocasted specimens were heat treated with a variant of the commercial heat treatment (T6). It consisted of a solution annealing at 548ºC during 6 hours, followed by water quenching and artificial ageing at 160ºC during 6 hours, which was also followed by water quenching.

The second set of test specimens was made of grey cast iron (ref. as SL 26) with the following chemical composition (in wt. %): Fe-3.18C-2.17Si-0.60Mn-0.7P-0.37Cr. A grey cast iron was chosen as a standard material to compare its performances with the thixocasted and heat-treated A356 alloy. The specimens made from SL 26 were fabricated using the sand casting procedure followed with heating at 550°C in order to eliminate residual stress in the material.

2.2. Structural and mechanical examinations

Microstructural and mechanical characterisation of tested materials included metallographic examinations with optical microscope (OM) and hardness and density measurements. Metallographic samples were prepared in a standard way applying grinding and polishing, whereas etching in Keller's solution (the mixture of 95 ml H_2O, 2.5 ml HNO_3, 1.5 ml HCl and 1 ml HF) was used to reveal the microstructure. Hardness measurements were carried out using a Vickers diamond pyramid indenter and a 10 kg load. Density of the samples was measured by Archimedes method.

2.3. Tribological tests

Tribological tests were carried out on the pin-on-disc tribometer under dry and lubricated sliding conditions in ambient air at room temperature (≈ 25°C). Cylindrical pins of tested materials having 2.5 mm diameter and 30 mm length were used as test samples. Disc (hereafter referred to as counter body) of 100 mm diameter and 10 mm thickness was made of nodular grey cast iron (220 HV 10). This material was chosen as a standard piston ring material with specification according to the ISO standard (Subclass Code MC 53) [10]. Surface roughness of pins and the counter body was approximately R_a = 0.5 and 0.3 μm, respectively.

For dry sliding condition tests, before and after testing, both the pin and the counter body were degreased and cleaned with benzene. Pins were weighed with an accuracy of 10^{-4} g before and after each test to calculate the mass loss. The value of friction force was monitored during the test and through data acquisition system stored in the PC, enabling the calculation of friction coefficient. Tests were carried out at selected test conditions: constant sliding speed of 1 m/s, constant sliding distance of 5000 m and 5 different normal loads. Taking into account the contact area of approximately 5 mm^2, the specific load (in MPa) was calculated as normal load divided with contact area.

For lubricated sliding condition tests standard motor oil was used (ACEA E3, SAE 15W-40). The temperature of oil was monitored and maintained constant at 60 ºC during the tests. Only the value of friction force was monitored during the lubricated sliding condition tests. Normal load was constant and had the value of 30 N, i.e. 6 MPa. The value of sliding speed was varied from 0.22 to 4.62 m/s (all together 12 different values), while the test duration was constant (15 minutes). Test duration was selected according to the pre-tests, in order to provide steady-state values of friction coefficient.

3. Results and discussion

3.1. Structural and mechanical examinations

The results of metallographic investigation of the thixocasted and heat--treated Al-Si alloy (Thixo T6) are illustrated in Fig. 1. The microstructure of Thixo T6 consists mainly of elliptical, aluminium rich, primary particles. During heat treatment, primary particles became larger and the entrapment of an eutectic phase within the primary particles took place (Fig. 1a). Silicon particles appeared as elliptical nodules (with a size 1.5 – 5 μm) and large irregular plates, statistically distributed in eutectic phase among large primary aluminium particles (Fig. 1b), and in the form of rows and clusters (details A and B in Fig. 1b), at rosette parts boundaries.

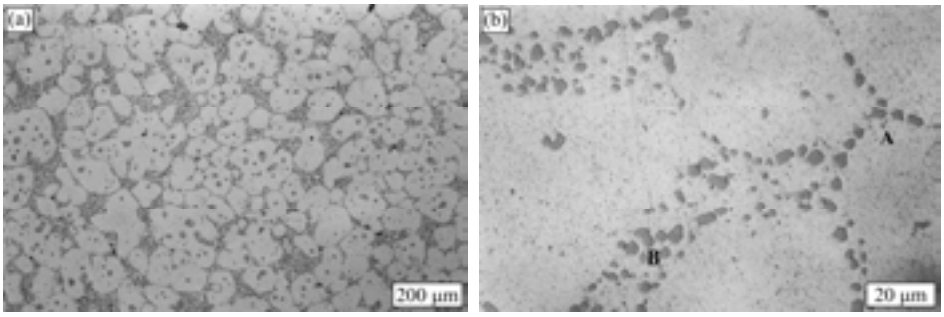

Fig. 1. OM microphotograph of etched Thixo T6 microstructure

The values of hardness were 121 and 254 HV 10 for Thixo T6 and SL 26 material, respectively, while the density of tested materials were 2.70 and 7.22 g/cm^3 for Thixo T6 and SL 26, respectively. At least six measurements were made for each specimen in order to eliminate possible segregation effects and to get a representative values.

3.2. Tribological tests

In order to achieve a higher confidence level in evaluating dry sliding conditions test results, three or more replicate tests were run for all the tested

materials. The results indicate good repeatability of the wear and friction results. Obtained results of the tested materials mass loss, for different specific loads, are shown as a function of sliding distance in the form of the comparative wear curves (Fig. 2). Wear curves were formed with the following method: the mass of all cylindrical pins was measured at the beginning of the test and at each pause in the testing (after 250, 500, 1000, 2000, 3000, 4000 and 5000 m), so the mass loss could be calculated for the mentioned sliding distances.

The wear curves of tested materials were in correlation with the theoretical ones. The amount of worn material increased with increasing of the specific load. From the shape of the wear curves it could be noticed that the run-in period was very short or did not exist at all. Almost from the beginning of the tests there was a steady-state wear in which the dependence of the mass loss from the sliding distance could be approximated as linear.

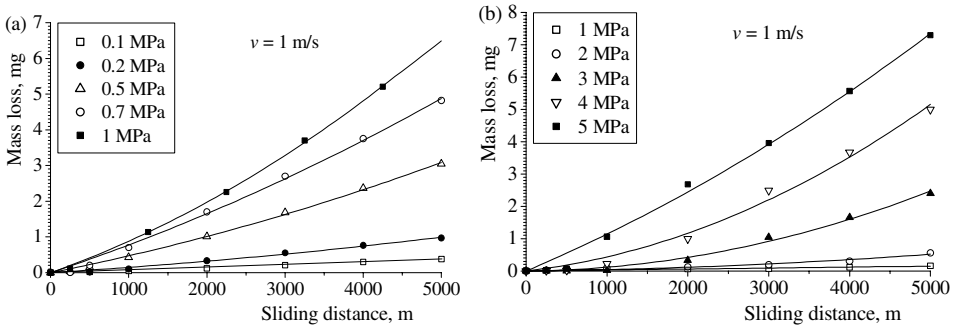

Fig. 2. The wear curves of: a) Thixo T6 material and b) SL 26 material

The wear rates (calculated for the steady-state period) of tested materials at different specific loads are presented in Fig. 3. The tendency for all materials was the same, i.e. with the increase of specific load the wear rate also increases. The Thixo T6 showed significantly higher wear rates than SL 26, almost two orders of magnitude (Fig. 3a).

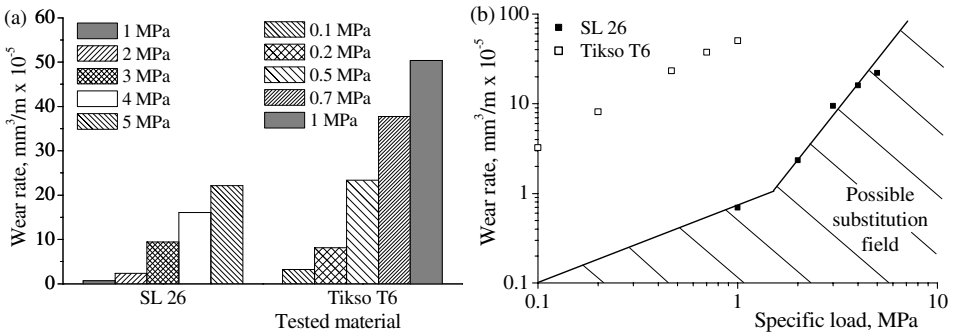

Fig. 3. The wear rates of tested materials for different specific loads

Presence of the critical load at which the wear rate abruptly increases, indicating the transition of wear regime, was noticed for SL 26 material. The possibility of grey cast iron (SL 26) substitution with Thixo T6 material, from the aspect of adhesion wear resistance, is shown in the form of log-log scale diagram (Fig. 3b). The dependence of the wear rate from the specific load for the grey cast iron is represented with two straight lines that divide the diagram into two fields: field of the materials that could and that could not be adequate substitution for grey cast iron. From Fig. 3b, it can be noticed that Thixo T6 did not enter the possible substitution field.

The coefficient of friction values of tested materials did not change significantly with the change of specific load, and one mean value per material could be accepted for the whole applied load interval. The values of coefficient of friction were 0.32 and 0.53 for Thixo T6 and SL 26 material, respectively. The attained friction coefficient value of the grey cast iron was in expected range for metals in dry sliding conditions. The relatively low friction coefficient value of the Thixo T6 material is due to the fact that at applied specific load pin surfaces of this material start to deform plastically and to flow (this was confirmed with optical observation, Fig. 4a).

Condition of pin contact surfaces was observed during the tests as well as at the end of tests and recorded with a camera (Fig. 4). Plastic flow of material on the surface of some pins was noticed. This plastic flow at Thixo T6 material was present, more or less intensive depending on the specific load, for the whole applied load interval (Fig. 4a), except for the lowest applied load of 0.1 MPa. For the SL 26 material, there was no noticed plastic deformation, for the whole applied load interval, even for the highest applied load of 5 MPa (Fig. 4b).

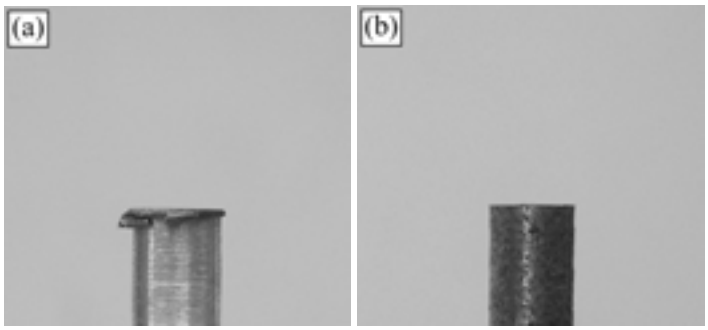

Fig. 4. The appearance of the pin contact surface of tested materials at the end of testing: a) Thixo T6 at 0.7 MPa and b) SL 26 at 5 MPa

The values of applied loads for SL 26 were similar to the average values that occur in cylinders of the gasoline internal combustion engines, compressors, and other piston machines. Good load bearing characteristics of grey cast iron was expected, since it is a standard material for cylinder blocks.

Tribological tests in lubricated sliding conditions were additionally done, in order to simulate the working condition in cylinders of the gasoline internal combustion engines, compressors, and other piston machines. The parameters that were taken into account were normal load, sliding speed, and lubricant type and temperature. The obtained dependence of the friction coefficient from sliding speed, for tested materials, is shown in Fig. 5.

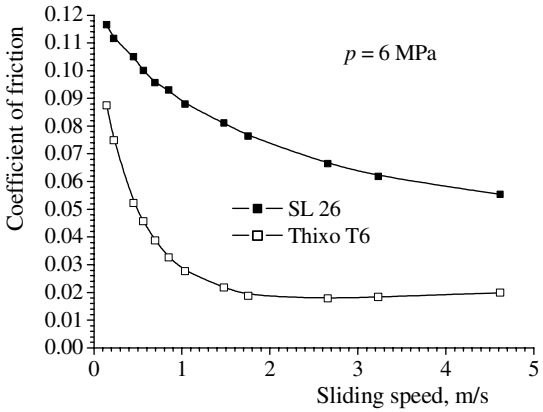

Fig. 5. Dependence of the friction coefficient from the sliding speed, for tested materials

The obtained values of the coefficient of friction indicate that a boundary lubrication condition was maintained. From Fig. 5, it can be noticed that, for investigated conditions, for SL 26 material, the coefficient of friction decreases with the increase of sliding speeds, while, for Thixo T6 material, the coefficient of friction decreased up to the value of the sliding speed of app. 3 m/s, and than it starts to increase with the increase of sliding speed. This was in accordance with the Stribeck curve. For all applied sliding speeds, the value of the friction coefficient was lower for Thixo T6 than for SL 26 material. Visual inspection of samples did not show any plastic deformation on either of the tested materials.

Obtained results suggest that, from the aspect of friction in lubricated sliding condition, Thixo T6 material could be an adequate substitution for grey cast iron (SL 26) in cylinders of the piston machines. Since these tests were just initial, further investigation should be done in a reciprocating sliding lubricated condition, with wear measurements as well.

4. Conclusion

Grey cast iron was chosen as a standard material for cylinders of the gasoline internal combustion engines, compressors, and other piston machines. In order to find an adequate substitution for grey cast iron, the structural,

mechanical and tribological properties of thixocasted and heat-treated hypoeutectic Al-Si alloy A356 was investigated.

The results of tribological tests under dry sliding conditions showed that the wear rates of the thixocasted and heat treated Al-Si alloy were almost two orders of magnitude higher than that of grey cast iron. Also, Al-Si alloy did not satisfy load bearing capacity criteria for the investigated load interval, and plastic flow of the material occurs. These results indicate that investigated Al-Si alloy has low adhesion wear resistance and could not be used for the same purposes, in dry sliding condition, as grey cast iron.

On the other side, under lubricated sliding conditions, when boundary lubrication was achieved, thixocasted and heat-treated Al-Si alloy showed comparable characteristics with grey cast iron. The coefficient of friction was lower and no plastic deformation occurs, i.e. these preliminary results indicate that investigated Al-Si alloy could be a possible substitution for grey cast iron in boundary lubrication conditions.

References

[1] A. Lowe, K. Ridgway, I. McCarthy, H. Atkinson, An evaluation model for determining the business process benefits of thixoforming, Proceedings of the Institution of Mechanical Engineers, 214B (2000) 11–23.

[2] Z. Fan, Semisolid metal processing, International Materials Reviews, 47 (2002) 49–85.

[3] P. Kapranos, D.H. Kirkwood, H.V. Atkinson, J.T. Rheinlander, J.J. Bentzen, P.T. Toft, C.P. Debel, G. Laslaz, L. Maenner, S. Blais, J.M. Rodriguez-Ibabe, L. Lasa, P. Giordano, G. Chiarmetta, A. Giese, Thixoforming of an automotive part in A390 hypereutectic Al-Si alloy, Journal of Materials Processing Technology, 135 (2003) 271–277.

[4] C.G. Kang, H.K. Jung, A study on Solutions for Avoiding Liquid Segregation Phenomena in Thixoforming Process: Part II. Net Shape Manufacturing of Automotive Scroll Component, Metallurgical and Materials Transactions, 32B (2001) 129–136.

[5] A. Vencl, I. Bobić, Z. Mišković, Effect of thixocasting and heat treatment on the tribological properties of hypoeutectic Al-Si alloy, Wear, 264 (2008) 616–623.

[6] A.P. Druschitz, T.E. Prucha, A.E. Kopper, T.A. Chadwick, Mechanical Properties of High Performance Aluminum Castings, SAE Technical Paper 2001-01-0406.

[7] E.R. de Freitas, E.G. Ferracini Júnior, V.P. Piffer, M. Ferrante, Microstructure, Material Flow and Tensile Properties of A356 Alloy Thixoformed Parts, Materials Research, 7 (2004) 595–603.

[8] E. Cerri, E. Evangelista, S. Spigarelli, P. Cavaliere, F. DeRiccardis, Effects of thermal treatments on microstructure and mechanical properties in a thixocast 319 aluminum alloy, Materials Science and Engineering A, 284 (2000) 254–260.

[9] L. Lasa, J.M. Rodriguez-Ibabe, Effect of composition and processing route on the wear behaviour of Al–Si alloys, Scripta Materialia, 46 (2002) 477–481.

[10] --, ISO 6621-3:2000 Internal Combustion Engines – Piston Rings – Part 3: Material Specifications, 2000.

Manuscript received by Editorial Board, February 26th, 2010

Własności tribologiczne stopu Al-Si A356 po obróbce cieplnej

S t r e s z c z e n i e

Przedstawiono wyniki badań strukturalnych, mechanicznych i tribologicznych stopu hipoeutektycznego Al-Si A356 (EN-AlSi7 Mg0,3). Wyniki testów tribologicznych zostały porównane z rezultatami uzyskanymi dla żeliwa szarego. W testach użyto stanowiska badawczego typu trzpień–tarcza. Badania obejmowały styk smarowany i niesmarowany dla szeregu wartości obciążenia i prędkości. Stwierdzono, że bez smarowania badany stop nie wykazuje pozytywnych własności z powodu występujących odkształceń plastycznych.

W styku smarowanym badany stop wykazał niski współczynnik tarcia i brak odkształceń plastycznych.

SCIENTIFIC PROBLEMS
OF MACHINES OPERATION
AND MAINTENANCE
3 (159) 2009

KLAUDIUSZ MIGAWA*

Semi-Markov model of the availability of the means of municipal transport system

Keywords

Transport system, municipal transport, semi-Markov model, technological object availability.

Słowa kluczowe

System transportowy, komunikacja miejska, model semi-Markowa, gotowość obiektu technicznego.

Summary

The article presents a method of designing the availability of technological objects used in complex operational systems with the assistance of a theory pertaining to semi-Markov processes. The complete consideration was presented based on the chosen authentic system of transport means operation – municipal bus transport system in a chosen urban complex. Direct realisation of transport goals of the municipal transport system is undertaken by a utilisation subsystem comprised of elementary subsystems of the operator – transport means (driver – bus) type, the availability of which significantly influences the possibility of appropriate realisation of these goals.

In order to build a model of the availability of transport means, significant operational states of the operational process were designed and a division and reduction of the number of states was done taking into consideration the criterion availability for operation. Based on this, both event-based and mathematical models of the process of transport means operation were built, assuming that the mathematical model of the process of transport means operation constitutes a homogenous

* University of Technology and Life Sciences, Department of Machine Maintenance, ul. Prof. S. Kaliskiego 7, 85-789 Bydgoszcz, Poland, e-mail: km@karor.com.pl

semi-Markov process. Then, for the operational data obtained from the testing of authentic operational process, limit values of the availability factor for the delineated levels of transport means availability in municipal transport system were defined.

This article presents a way to define the availability of a single technological unit – transport means, based on the constructed semi-Markov model of operational process used in a utilisation subsystem of the tested transport means system. The presented model for designing the availability of transport means is part of a decision-making model of controlling transport system availability created within the framework of a larger research project.

1. Introduction

Technological object (element or system) availability is the object's feature, which is characteristic from the point of view of the possibility of timely obtaining or maintaining the state of efficiency (facilitating the realisation of goals) [6, 8, 10, 11]. The term 'availability' pertains to the systems characterised by the necessity of quick reaction in emergency situations; such systems include the military, police, ambulance service, fire department, as well as transport systems. In such systems, whenever there is a goal in an emergency situation, an individual or a team of individuals with their assigned technological objects attempts its *immediate* realisation.

A unique type of transport system is the municipal bus transport system with the main goal of passenger transport. The frequency of rides and a complex number of persons on board determine the size of the transport goals, in an assigned period of time, on a defined route. In systems of this type, the direct implementation of passenger transport remains the responsibility of the utilisation subsystem comprised of elementary subsystems of the operator – transport means (driver – bus) type. It is on the availability of these subsystems that the possibility of appropriate implementation of transport goals depends. Availability of transport means remains at an appropriate level, as a result of the repair processes implemented in the utilisation subsystem by technological support units and in the efficiency implementation in repair posts at the bus depot. The above results in the availability of transport system being dependent on the possibility of correct control of the process of operation is realised both in the utilisation and efficiency implementation subsystems.

This article presents a way of defining availability of a single technological object – means of transport, based on the built semi-Markov model of operational process realised in the utilisation subsystem of the tested municipal transport system. The model of determining the availability of transport means presented here is a part of a decision-making model of controlling transport system availability created within a larger research project. In the following stages, a model for determining utilisation subsystem availability comprised of N number of transport means combined with an appropriate structure will be created, together with a model of defining and the evaluating of the availability of an efficiency implementation subsystem.

2. Event-based operation process model

An event-based model of an operation and maintenance process was built on the basis of the analysis of the operation and maintenance states space and the operation and maintenance events regarding the technical objects being operated and maintained within a real transport system under analysis. Each of the operated and maintained technical object may, at any moment *t*, stay in only one of the distinguished states, forming a finite set of operation and maintenance states of an object. The following significant operation and maintenance states have been distinguished in the analysed operation and maintenance process model:

- S_1 – stopover at bus depot parking space,
- S_2 – repair at bus depot parking space,
- S_3 – carrying out of the transport goal,
- S_4 – fuel intake between transport peak hours,
- S_5 – repair by technical support unit without losing a trip,
- S_6 – repair by technical support unit with losing a trip,
- S_7 – awaiting the start of task realisation after technical support repair,
- S_8 – emergency exit,
- S_9 – technical object repair at the efficiency implementation subsystem posts.

Afterwards, the possible transitions between the distinguished operation and maintenance states were determined. It was the basis for making a graph of the operation and maintenance state changes, as presented in the Fig. 1.

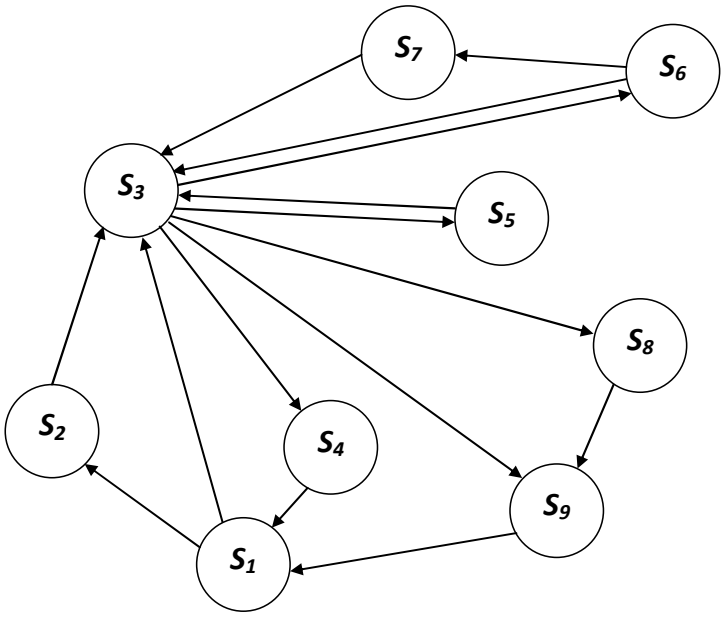

Fig. 1. Directed graph representing the transport means operation process
Rys. 1. Graf skierowany odwzorowania procesu eksploatacji środków transportu

3. Semi-Markov model of the availability of transport means

In general, the availability of technological object to realise the assigned goal is described as a technological object feature that characterises it from the point of view of the possibility of timely obtaining and maintaining the state of efficiency (facilitating the realisation of the goal) at moment t or during time range τ_r of time reserve for supplies and/or object repair.

In this paper, the value of technological object availability is defined for three selected levels:

- First level availability $G_{OT(1)}^{24}$ is determined for objects, which at any given moment t are efficient and supplied; in case of the tested system, it pertains to technological objects which realise the assigned goal or await the beginning of goal realisation at the parking place of the bus depot or following repair done by technical support unit.
- Second level availability $G_{OT(2)}^{24}$ is additionally assigned for efficient technological objects which are to be supplied, e.g. in fuel; however, the supply process will be realised in $T_z \leq \tau_z$ shorter than the period of time reserve for supplying technological objects without losing a trip, i.e. during the breaks between trips determined by the schedule of transport goals realisations (bus schedule).
- Third level availability $G_{OT(3)}^{24}$ is additionally determined for inefficient technological objects which were damaged at the parking place of the bus depot while awaiting the realisation of the transport goal or en route while realising the transport assignment but were repaired by bus depot technicians or technical support unit in $T_u \leq \tau_u$ time shorter than the period of time reserve without losing a trip, i.e. during the breaks between trips determined by the schedule of transport goals (bus schedule).

In the examined model, it is assumed that both the supplies of the technological object during time reserve τ_z and the repair during time reserve τ_u do not stop the goal from being realised and, at the same time, do not make it necessary to substitute the supplied or repaired object with a different one (reserve object).

3.1. Mathematical model of the operation process

Using the semi-Markov processes in the mathematical modelling of the operation process, the following assumptions were put forward:

- The modelled operation process has a finite number of states S_i, $i = 1,2,\ldots,9$.
- The random process $X(t)$ being the mathematical model of the operation process is a homogenous process.
- At moment $t = 0$, the process finds is in state S_3 (the initial state is state S_3).

The homogenous semi-Markov process is unequivocally defined when initial distribution and its kernel are given. From our assumptions and based on the directed graph shown in Figure 1, the initial distribution $p_i(0) = P\{X(0) = i\}, \quad i = 1,2,...,9$ takes the following form:

$$p_i(0) = \begin{cases} 1 & when \quad i = 3 \\ 0 & when \quad i \neq 3 \end{cases} \tag{1}$$

whereas, the kernel of process *Q(t)*:

$$Q(t) = \begin{bmatrix} 0 & Q_{12}(t) & Q_{13}(t) & 0 & 0 & 0 & 0 & 0 & 0 \\ 0 & 0 & Q_{23}(t) & 0 & 0 & 0 & 0 & 0 & 0 \\ 0 & 0 & 0 & Q_{34}(t) & Q_{35}(t) & Q_{36}(t) & 0 & Q_{38}(t) & Q_{39}(t) \\ Q_{41}(t) & 0 & 0 & 0 & 0 & 0 & 0 & 0 & 0 \\ 0 & 0 & Q_{53}(t) & 0 & 0 & 0 & 0 & 0 & 0 \\ 0 & 0 & Q_{63}(t) & 0 & 0 & 0 & Q_{67}(t) & 0 & 0 \\ 0 & 0 & Q_{73}(t) & 0 & 0 & 0 & 0 & 0 & 0 \\ 0 & 0 & 0 & 0 & 0 & 0 & 0 & 0 & Q_{89}(t) \\ Q_{91}(t) & 0 & 0 & 0 & 0 & 0 & 0 & 0 & 0 \end{bmatrix} \tag{2}$$

where:

$$Q_{ij}(t) = P\{X(\tau_{n+1}) = j, \tau_{n+1} - \tau_n \leq t \,|\, X(\tau_n) = i\}, \quad i, j = 1,2,...,9 \tag{3}$$

means that the state of semi-Markovian process and the period of its duration depends solely on the previous state, and does not depend on earlier states and periods of their duration, where $\tau_1, \tau_2, \ldots, \tau_n, \ldots$ are arbitrary moments in time, so that $\tau_1 < \tau_2 < \ldots < \tau_n < \ldots$;
as well as

$$Q_{ij}(t) = p_{ij} \cdot F_{ij}(t) \tag{4}$$

where:

$$p_{ij} = \lim_{t \to \infty} p_{ij}(t) \tag{5}$$

p_{ij} – means that the conditional probability of transfer from state S_i to state S_j,

$$p_{ij}(t) = P\{X(t) = j | X(0) = i\} \tag{6}$$

as well as

$$F_{ij}(t) = P\{\tau_{n+1} - \tau_n \le t | X(\tau_n) = i, X(\tau_{n+1}) = j\}, \quad i, j = 1,2,...,9 \tag{7}$$

is a distribution function of random variable Θ_{ij} signifying the period of duration of state S_i, under the condition that the next state will be state S_j.

3.2. Availability of transport means

In general, availability of technological objects determined based on the semi-Markov operation process model is defined as the sum of limit probabilities p_i^* of being in states belonging to the set of availability states

$$G = \sum_i p_i^*, \quad dla \quad S_i \in S_G, \quad i = 1,2,...,9 \tag{8}$$

In order to assign the values of limit probabilities p_i^* of staying in the states of semi-Markovian model of transport means operation, based on the directed graph shown in Figure 1, the following matrix P was created of the states change probabilities in process $X(t)$:

$$P = \begin{bmatrix} 0 & p_{12} & p_{13} & 0 & 0 & 0 & 0 & 0 & 0 \\ 0 & 0 & 1 & 0 & 0 & 0 & 0 & 0 & 0 \\ 0 & 0 & 0 & p_{34} & p_{35} & p_{36} & 0 & p_{38} & p_{39} \\ 1 & 0 & 0 & 0 & 0 & 0 & 0 & 0 & 0 \\ 0 & 0 & 1 & 0 & 0 & 0 & 0 & 0 & 0 \\ 0 & 0 & p_{63} & 0 & 0 & 0 & p_{67} & 0 & 0 \\ 0 & 0 & 1 & 0 & 0 & 0 & 0 & 0 & 0 \\ 0 & 0 & 0 & 0 & 0 & 0 & 0 & 0 & 1 \\ 1 & 0 & 0 & 0 & 0 & 0 & 0 & 0 & 0 \end{bmatrix} \tag{9}$$

Limit probability p_i^* of staying in states of semi-Markov process were assigned on the basis of the limit theorem for semi-Markovian processes [2, 7]:

If hidden Markov chain in semi-Markovian process with finite state S set and continuous type kernel contains one class of positive returning states such that for each state $i \in S, f_{ij} = 1$ and positive expected values $E(\Theta_i), i \in S$ are finite, limit

$$p_i^* = \lim_{t\to\infty} p_i(t) = \frac{\pi_i \cdot E(\Theta_i)}{\sum_{i\in S} \pi_i \cdot E(\Theta_i)} \tag{10}$$

exist where probabilities $\pi_i, i \in S$ constitute a stationary distribution of a hidden Markov chain, which fulfils the simultaneous linear equations

$$\sum_{i\in S} \pi_i \cdot p_{ij} = \pi_j, \quad j \in S, \quad \sum_{i\in S} \pi_i = 1. \tag{11}$$

In order to determine the availability of transport system objects (transport means) based on the semi-Markov operation process model, the operational states of the technological object should be divided into availability states S_G and non-availability state S_{NG} of the object to realise the assignment. Technological object availability states are states during which the object, including the operator, remains in the operation system, and is efficient and supplied or will be repaired and/or supplied in a period of time shorter than the time reserve which is to serve the purpose. Non-availability states are states in which the object or the operator remains outside the operation system (efficient or inefficient), as well as when an inefficient and/or unsupplied object remains in the operation system.

In the presented model, for each level of availability the following technological object availability states were defined:

– for the first level:
  State S_1 – stopover at bus depot parking space,
  State S_3 – carrying out of the transport goal,
  State S_7 – awaiting the start of task realisation after technical support repair,
– for the second level:
  State S_1 – stopover at bus depot parking space,
  State S_3 – carrying out of the transport goal,
  State S_7 – awaiting the start of task realisation after technical support repair,
  State S_4 – intake between transport peak hours,
– for the third level:
  State S_1 – stopover at bus depot parking space,
  State S_3 – carrying out of the transport goal,
  State S_7 – awaiting the start of task realisation after technical support repair,
  State S_4 – intake between transport peak hours,
  State S_2 – repair at bus depot parking space,
  State S_5 – repair by technical support unit without losing a trip.

Then, with the use of the MATHEMATICA software, the limit probability p_i^* of staying in states of semi-Markov process and the availability of technological objects of the transport system were determined, defined by the following dependencies:

$$G_{OT(1)}^{24} = p_1^* + p_3^* + p_7^* \tag{12}$$

$$G_{OT(1)}^{24} = \frac{(p_{34}+p_{38}+p_{39})\cdot\overline{\Theta_1}+\overline{\Theta_3}+p_{36}\cdot p_{67}\cdot\overline{\Theta_7}}{\left[(p_{34}+p_{38}+p_{39})\cdot\left(\overline{\Theta_1}+p_{12}\cdot\overline{\Theta_2}\right)\right]+\overline{\Theta_3}+p_{34}\cdot\overline{\Theta_4}+p_{35}\cdot\overline{\Theta_5}+\left[p_{36}\cdot\left(\overline{\Theta_6}+p_{67}\cdot\overline{\Theta_7}\right)\right]+p_{38}\cdot\overline{\Theta_8}+(p_{38}+p_{39})\cdot\overline{\Theta_9}} \tag{13}$$

$$G_{OT(2)}^{24} = p_1^* + p_3^* + p_7^* + p_4^* \tag{14}$$

$$G_{OT(2)}^{24} = \frac{(p_{34}+p_{38}+p_{39})\cdot\overline{\Theta_1}+\overline{\Theta_3}+p_{34}\cdot\overline{\Theta_4}+p_{36}\cdot p_{67}\cdot\overline{\Theta_7}}{\left[(p_{34}+p_{38}+p_{39})\cdot\left(\overline{\Theta_1}+p_{12}\cdot\overline{\Theta_2}\right)\right]+\overline{\Theta_3}+p_{34}\cdot\overline{\Theta_4}+p_{35}\cdot\overline{\Theta_5}+\left[p_{36}\cdot\left(\overline{\Theta_6}+p_{67}\cdot\overline{\Theta_7}\right)\right]+p_{38}\cdot\overline{\Theta_8}+(p_{38}+p_{39})\cdot\overline{\Theta_9}} \tag{15}$$

$$G_{OT(3)}^{24} = p_1^* + p_3^* + p_7^* + p_4^* + p_2^* + p_5^* \tag{16}$$

$$G_{OT(3)}^{24} = \frac{(p_{34}+p_{38}+p_{39})\cdot\left(\overline{\Theta_1}+p_{12}\cdot\overline{\Theta_2}\right)+\overline{\Theta_3}+p_{34}\cdot\overline{\Theta_4}+p_{35}\cdot\overline{\Theta_5}+p_{36}\cdot p_{67}\cdot\overline{\Theta_7}}{\left[(p_{34}+p_{38}+p_{39})\cdot\left(\overline{\Theta_1}+p_{12}\cdot\overline{\Theta_2}\right)\right]+\overline{\Theta_3}+p_{34}\cdot\overline{\Theta_4}+p_{35}\cdot\overline{\Theta_5}+\left[p_{36}\cdot\left(\overline{\Theta_6}+p_{67}\cdot\overline{\Theta_7}\right)\right]+p_{38}\cdot\overline{\Theta_8}+(p_{38}+p_{39})\cdot\overline{\Theta_9}} \tag{17}$$

Then, using the above formulas, values of availability of transport means used in the tested municipal bus transport system were defined (Table 1).

Table 1. Values of availability of transport means used in the tested municipal bus transport system

Tablica 1. Wartości gotowości środków transportu eksploatowanych w systemie autobusowej komunikacji miejskiej

$G_{OT(1)}^{24}$	$G_{OT(2)}^{24}$	$G_{OT(3)}^{24}$
0,8444	0,8509	0,8518

4. Conclusion

Using semi-Markov processes for the modelling of the operational process of transport means facilitates the determination of transport means availability in case of time periods between changes of individual process states having arbitrary probability distribution and transfer to the following state depends only on the current process state.

Availability of technological objects (transport means) used in the municipal bus transport system, determined on the basis of semi-Markovian operational process model, depends directly on the values of limit probabilities

pi^* of being at the states of the analysed process, and indirectly on the values of probabilities of transfers between process states p_{ij} (values of the elements of matrix P) as well as values of conditional duration periods of process states $\overline{\Theta}_{ij}$ (values of matrix Θ).

Change of the values of probabilities p_{ij} as well as duration periods $\overline{\Theta}_{ij}$ causes the change of the values of transport system technological objects availability G_{OT}. Values of availability of transport system technological objects G_{OT} depend on many factors:

- In case of the first level:
  - The reliability of the technological objects in use,
  - The efficiency of repair processes carried out at logistics subsystem posts and by technical support units,
- In case of the second level:
  - The number of fuel supply posts in the subsystem,
  - The efficiency of the subsystem fuel intake posts,
  - The values of the time reserve for supply of technological objects without losing a trip,
- In case of the third level:
  - The number of technical support units,
  - Equipping the technical support units with tools and devices used in technological object repair ensuring high efficiency of the performed repairs,
  - The serviceability and repair efficiency of technological objects,
  - The values of time reserve for technological object repair without losing a trip.

Values of transport means availability obtained on the basis of operational data presented in Table 1 are not high. However, one should take into consideration the fact that high availability of the utilisation subsystem comprised of N number of transport means may be obtained as a result of using the appropriate structure which integrates technological objects and numbers of reserve objects. The model of defining the availability of the utilisation subsystem comprised of N transport means will be prepared at future stages of the work conducted.

References

[1] Bobrowski D.: Modele i metody matematyczne w teorii niezawodności. Warszawa, WNT, 1985.

[2] Grabski F.: Semi-markowskie modele niezawodności i eksploatacji, Polska Akademia Nauk, Instytut Badań Systemowych, seria: Badania systemowe, tom 30, Warszawa 2002.

[3] Grabski F., Jaźwiński J.: Funkcje o losowych argumentach w zagadnieniach niezawodności, bezpieczeństwa i logistyki, WKiŁ, Warszawa, 2009.
[4] Iosifescu M.: Skończone procesy Markowa i ich zastosowanie, PWN, Warszawa, 1988.
[5] Jaźwiński J., Grabski F.: Niektóre problemy modelowania systemów transportowych, Instytut Technologii Eksploatacji, Warszawa–Radom, 2003.
[6] Kołowrocki K., Woropay M., Modelowanie gotowości systemu transportu autobusowego. Materiały Szkoły Zimowej, Szczyrk, 2001.
[7] Koroluk V.S., Turbin A. F.: Semi-Markov processes and their application, Naukova Dumka, Kiev, 1976.
[8] Praca zbiorowa pod redakcją J.M. Migdalskiego, *Inżynieria niezawodności. Poradnik*. Warszawa, Wydawnictwo ZETOM, 1992.
[9] Woropay M., Migawa K.: *Markov model of the operational use process in an autonomous system*. Polish Journal of Environmental Studies, Vol. 16, No 4A, 2007.
[10] Woropay M., Szubartowski M., Migawa K.: *Model oceny i kształtowania gotowości operacyjnej podsystemu wykonawczego w systemie transportowym*. Wydawnictwo i Zakład Poligrafii Instytutu Technologii Eksploatacji, Radom, 2003.
[11] Żurek J., *Problemy gotowości techniki lotniczej*. Rozdział 13, Praca zbiorowa: Problemy badań i eksploatacji techniki lotniczej, Tom 2, Warszawa, Wydawnictwo ITWL, 1993.

Manuscript received by Editorial Board, November 15th, 2009

Semimarkowski model gotowości środków transportu systemu komunikacji miejskiej

S t r e s z c z e n i e

W artykule przedstawiono metodę wyznaczania gotowości obiektów technicznych, użytkowanych w złożonych systemach eksploatacji, z wykorzystaniem teorii dotyczącej procesów semi-Markowa. Całość rozważań przedstawiono na przykładzie wybranego rzeczywistego systemu eksploatacji środków transportu – systemu autobusowej komunikacji miejskiej w wybranej aglomeracji. Bezpośrednią realizacją zadań przewozowych systemu komunikacji miejskiej zajmuje się podsystem wykonawczy złożony z podsystemów elementarnych typu operator–środek transportu (kierowca–autobus), których gotowość w istotny sposób wpływa na możliwość prawidłowej realizacji tych zadań.

W celu zbudowania modelu gotowości środków transportu wyznaczono istotne stany eksploatacyjne procesu eksploatacji oraz dokonano podziału i redukcji liczby stanów ze względu na kryterium gotowości do działania. Na tej podstawie zbudowano zdarzeniowy oraz matematyczny model procesu eksploatacji środków transportu, zakładając, że matematycznym modelem badanego procesu eksploatacji jest jednorodny proces semi-Markowa. Następnie dla danych eksploatacyjnych, uzyskanych z badań rzeczywistego procesu eksploatacji, wyznaczono graniczne wartości współczynnika gotowości dla wyróżnionych poziomów gotowości środków transportu eksploatowanych w systemie komunikacji miejskiej.

W prezentowanej pracy przedstawiono sposób wyznaczania gotowości pojedynczego obiektu technicznego – środka transportu, na podstawie zbudowanego semimarkowskiego modelu procesu eksploatacji, realizowanego w podsystemie wykonawczym badanego systemu transportu miejskiego. Przedstawiony w pracy model wyznaczania gotowości środków transportu jest częścią składową opracowywanego w ramach szerszego projektu badawczego, decyzyjnego modelu sterowania gotowością systemu transportowego.

SCIENTIFIC PROBLEMS
OF MACHINES OPERATION
AND MAINTENANCE
3 (159) 2009

STANISŁAW DUER*

Creation of the servicing information to support the maintenance of a technical object with the use of three-value logic diagnostic information

Key words

Servicing system, expert systems, knowledge base, diagnostic information.

Słowa kluczowe

System obsługiwania, systemy ekspertowe, baza wiedzy, informacja diagnostyczna.

Summary

The paper presents a method to construct the structure of a system for servicing of reparable technical objects. In the method proposed, diagnostic information from an artificial neural network and expert knowledge were used. The manner of realisation of the servicing model of an object was presented. An important stage in the proposed method of the development of the structure of a system for servicing of an object is the way in which the internal structure of a complex object is converted together with its functional elements to the form of the object's servicing structure. The article also covers an analytical basis for the determination of servicing information (servicing expert knowledge) which organises the system for the servicing of a technical object. Analytical bases were presented of the process of restoration of the functional properties of the object of servicing.

* Koszalin University of Technology, Department of Mechanical Engineering, 15-17 Racławicka Str., 75-620 Koszalin, Poland, e-mail: stanislaw.duer@tu.koszalin.pl

1. Introduction

The state of the technical object changes during the exploitation from the nominal state for which this object was designed. As a result, the usability features decrease in time, which usually decreases the functionality and/or the quality of the object. Among the set of indexes which characterise the process of the usage presented in literature [4, 11], the two which reflect object's usability features best are the usage quality function ($F_C(t)$) and the usage quality ratio (F_C).

Usage function of the object ($F_C(t)$) describes quality of object's performances considering its purpose and characteristic.

The state of object is determined by the subset of its physical properties [1, 2, 11], which are significant concerning the tasks of the object.

The technical state of the object in a given time of the use determines the possibilities of the realisation of its required functions. It is determined by a subset of its physical properties [1, 2, 3, 7, 9, 11, 12, 13], which describe a given object. For practical reasons, to the states of the object in the diagnosing process, numerical values are assigned, which depend on the logic of the classification of the states applied. For divalent logic, these are states from set {1, 0}, where: "1" is the operational state, and "0" is the non-operational state. For the trivalent assessment of the classification of states [1, 2, 3, 4, 7], to the states of the object, states marked with the values from set {2, 1, 0}, were assigned, where: "2" – the state of full operation; "1" – the state of incomplete usability; "0" – the state of non-operation (defect).

The problem of the description of a technical object: "an incomplete usability state," which is presented among other things in the author's papers [3, 4, 5, 8]: technical diagnostics presents the basis and organisation of diagnostic inference in technical objects as the final element of diagnosing. The effect of diagnostic inferring is the determined (recognised) states of the object's functional elements, on the basis of which the object's resultant stage is determined. Diagnosis of a technical object can also be performed in divalent logic {1, 0} or trivalent logic {2, 1, 0}. The basis for the diagnosis of technical objects is constituted by possible changes of the values of output diagnostic signals (mainly in the analogue form, but also in other forms) from the object's functional elements. Divalent logic constitutes the basis for the application of the trivalent logic of the evaluation of the object's states. Changes of the values of diagnostic signals are only in the range of their permissible and boundary changes. The range of these changes for a given object is constant regardless of the type of the valence used for the determination of the object's states. Additionally, for trivalent logic, the range of changes was divided-determined: state {1}, state of incomplete usability.

The quality of the use of an object can be measured with two quantities [1, 2, 7, 9, 11, 13]: the use function of the object $F_C(t)$ and F_C index of the use function of the

object (Fig. 1). The values of function $F_C(t)$ are determined by the divergence between the actual state of the object in the space of the use features (ω), and the state of the usability in the nominal space of usability features (M_E) (Fig. 1). The nominal space of usability features (M_E) is determined by elementary nominal vectors of the object's usability function $F_C(e_{i,j})$.

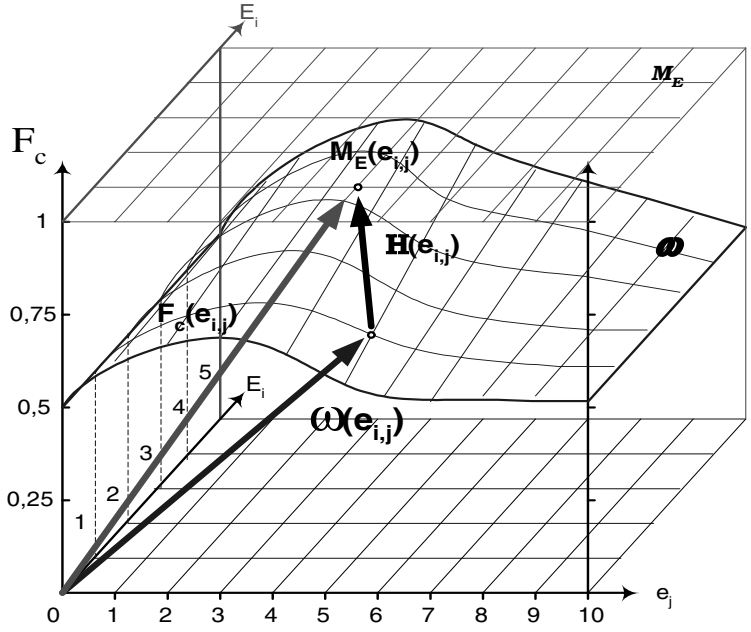

where: ω – the surface of actual usability features of the object; M_E – the surface of the nominal usability features of the object; $F_c(e_{i,j})$ – the value of use function; $\omega(e_{i,j})$ – vector of actual diagnostic signal; $H(e_{i,j})$ – vector of differential metric of diagnostic signal.

Fig. 1. Distribution of changes of object's states during operating time (example)
Rys. 1. Mapa przestrzenna zmiany stanów obiektu w czasie użytkowania (przykład)

The elementary vectors of the object's usability function $F_C(e_{i,j})$ can have various forms (measurable and other ones), and can have different dimensions. Therefore, initiation disproportion that is too large must be smoothed away between the values of these vectors of the object's usable function $F_C(e_{i,j})$ in particular dimensions. One of reliable methods of the transformation of input data (signals), and which is at the same time an effective method, is the normalisation of data in such a manner so that the values should be in the range (0, 1) after the conversion. A normalisation of the metric of any vector of the object's usability function $F_C(e_{i,j})$ consists in a redefinition of k^{th} components of vector $[F_C(e_{i,j})]$ by making calculations in compliance with the following dependence:

$$F_c\left(e_{i,j}\right)=\frac{F_c\left(e_{i,j}\right)_k}{\sqrt{\sum_{k=1}^{K}\left(F_c\left(e_{i,j}\right)\right)_k^2}} \tag{1}$$

where: k – subset of physical properties which determine elementary use functions of j^{th} element in i^{th} unit of the object

Realisation of the object's prevention is a transformation of the information described with diagnostic plane $\{\omega(e_{i,j})\}$ to the level of the servicing information represented with plane $\{H(e_{i,j})\}$ [4, 5, 8]. A reproduction of the qualitative property of usability function F_C of the object in the servicing process on the example of $F_C(e_{i,j})$ is presented in (Fig. 1). It is evident from an analysis of the diagram of the refurbishing of the object present in (Fig. 1) that the vector of qualitative usability function F_C described with quantity $\{\omega(e_{i,j})\}$ during operation is subject to a deviation from nominal state $M_E(e_{i,j})$ by vector $H(e_{i,j})$.

The methods for the creation of a servicing knowledge base were verified using the example of a radar system.

2. The maintenance system for servicing of a radar system "Straight Flush Radar Vehicle."

In order to design the servicing system for an analogue class technical object, in this case it was an air-defence radar device [13], it was needed to determine the internal structure of serviced object and the set of preventive activities for the non-operational elements. The radar system-Straight Flush Radar Vehicle is a part of a surface–to–air–missiles system (SA-6 "GAINFUL"). The purpose of the radar system is to fight air targets (aircrafts, helicopters, rockets, drone vehicles), as well as ground and water targets in the range of missiles. The radar system "Straight Flush Radar Vehicle" presented in Fig. 2 detects (determines the azimuth, distance and height) and controls the air fight. The antiaircraft set is adapted to work regardless of the time of the year and the day, in temperatures from -40°C to +50°C, with a relative humidity of 90 per cent and the wind speed up to 20 m/s.

The radar system-Straight Flush Radar Vehicle is characterised by a high resistance to climactic and natural factors. (SA-6 GAINFUL) system can be operated fully automatically as regards detection, identification, tracking, and raking of targets. The set is adapted to cooperation and coupling with four sources of external information. The radar can rake at the same time 1 target with 1 or 2 rockets fired within a span of 5 [sec] from one or two launchers.

The set considering the specificity of its function of the use (combating of air object) belongs to the group of technical equipment which is characterised by a high index of operational readiness. This class of technical object requires a specific approach as regards the maintenance of their fitness for use states. An optimal preventative strategy for this class of objects is an organisation of the operation of the object according to the state. This means that the technical object used is diagnosed on a continuous basis (state testing).

Fig. 2. The picture of an air-defence radar device of (SA-6) system
Rys. 2. Widok zestawu stacji radiolokacyjnej wykrywania i naprowadzania systemu (SA-6)

The diagnostic system recognises the states of the object and updates the user of the object about a given state. If an incomplete usability state {1} is identified in the object, then the regeneration of the object should begin. Therefore, the basis of the operation of an object in such a system is constituted by a reliable and effective diagnostic system.

The method presented in the present paper concerning the control of the exploitation of a technical object on the basis of its state was verified on the example of a reparable technical object, which is a radar system-Straight Flush Radar Vehicle. A functional and diagnostic analysis of the object was carried out for this purpose. A functional model was prepared and described of the object: a missile homing station of an antiaircraft missile set, which was presented in Fig 3. As a result of the described manner of the division of the object's internal structure, the object was subject to a three-level partition of its structure. As a consequence of this division of the internal structure (Fig. 3), seven functional assemblies were distinguished (E_1, E_2,…, E_7), and up to five basic elements – modules [1, 4, 5, 6] were distinguished in each one of them. As a result of the analysis carried out, a functional and diagnostic diagram was developed, on the basis of which a set of operational elements and a set of output (diagnostic) signals were established.

The method presented of the determination of diagnostic information (state evaluation) [1, 2, 3, 6, 7, 13] in the object examined can be realised with the aid of a module method, particularly when the object examined is a complex object. Then we examine the technical state of the elements-modules in the object on the lowest level of the analysed structure of the object, going "step by step." Diagnosis should begin with the low level of the structure, and should finish on the highest level of this structure, i.e. the object itself. For this purpose, the functional element was subject to an analysis on the second level of the diagnostic structure of the object, which is the functional assembly. For further determination of the diagnostic control (operational) information, assembly E_2: transmitter was chosen as an example.

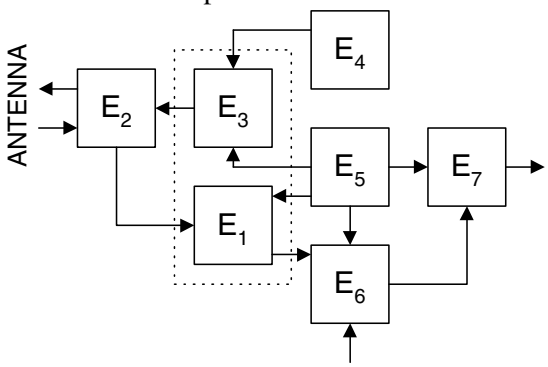

Where: E_1 – steering (synchronisation) unit, - E_2 – transmitter unit (channel I or channel II), E_3 – receiving unit, E_4 – permanent echo suppression unit, E_5 – display indicator unit, E_6 – precise display indicator unit, E_7 – electric power supply unit of the station.

Fig. 3. The functional scheme of air-defence radar device
Rys. 3. Schemat funkcjonalny zestawu stacji radiolokacyjnej wykrywania i naprowadzania

For the needs of the diagnosing process, a measuring track was designed for the diagnostic system. A properly designed measuring system [5] for the diagnostic system enables one to obtain a reliable measuring knowledge base for the diagnostic system $\{X(e_{i,j})$. The object's measuring information created in this manner constitutes the input information in the diagnosing system with a neural network [4, 5, 8, 10, 14, 15]. The results of measurements for chosen elements of the object are presented Fig. 4.

For the needs of the method presented, an effective diagnostic system [4, 5, 8] was built whose task is to recognise (classify) the object's states in trivalent logics {2, 1, 0}. The diagnostic system used in the tests was constructed on the basis of the measuring information obtained and DIAG diagnosing software. DIAG software is a specialist computer diagnostic programme developed for the needs of the method presented. The diagnostic information obtained during diagnosing in the form of the knowledge base $\{W(\varepsilon(e_{i,j}))\}$ constitutes the input information in the process of obtaining of the expert knowledge base which assists the maintenance of the technical object tested.

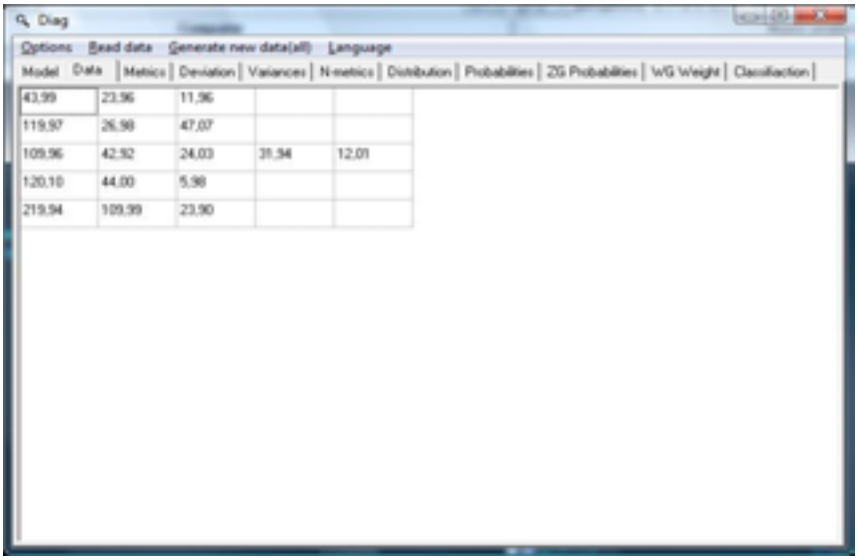

Fig. 4. Matrix of measures of diagnostic signals from the assembly E_2
Rys. 4. Ekran sygnałów diagnostycznych zespołu E_2

The final results obtained of diagnostic programme DIAG [8] were presented in the form of a table of states of the object (Table 1 and Fig. 5).

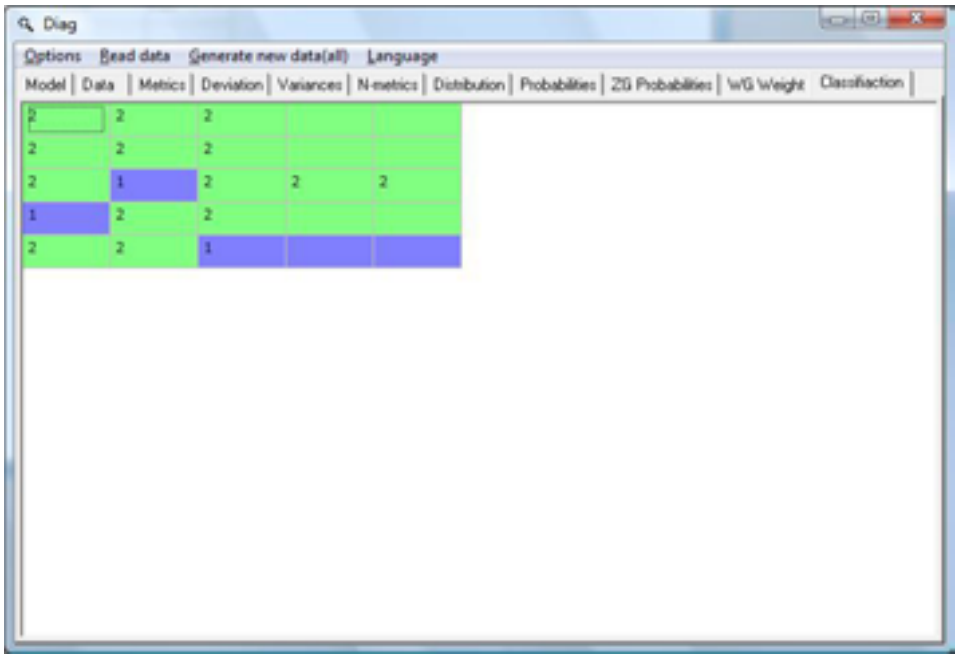

Fig. 5. The result form of DIAG programme "Table of object's states" of assembly E_2
Rys. 5. Postać wynikowa programu DIAG „Tablica stanów obiektu" dla zespołu E_2

Table 1. Value of states of assembly E_2
Tabela 1. Tabela stanu zespołu E_2

State of the assembly E_2	State of module	Vector of states $\varepsilon(e_i)$				
		e_1	e_2	e_3	e_4	e_5
0	2	2	2	2	∅	∅
	2	2	2	2	∅	∅
	1	2	1	2	2	2
	1	1	2	2	∅	∅
	1	2	2	1	∅	∅

where: Ø – lack of basic element: symbol which completes the size of the Table; {0,1,2} – states of the element

On the basis of the examination of the object's state, tables of states were determined for assembly E_2, and a comparison was made of the states [3, 7] with the model state, which is presented in Tables 2 and 3.

Table 2. Results of comparison of states of assembly E_2
Tabela 2. Wyniki porównania stanów zespołu E_2

Servicing levels	Servicing structure of assembly E_2					
1	⊗	⊗	⊗	⊗	⊗	⊗
	⊗	⊗	⊗	⊗	⊗	⊗
	⊗	1	⊗	⊗	⊗	⊗
	1	⊗	⊗	⊗	⊗	⊗
	⊗	⊗	1	⊗	⊗	⊗

where: ⊗ – lack of basic element: symbol which completes the size of the Table

Table 3. Set of servicing information of assembly E_2
Tabela 3. Zbiór informacji obsługowej zespołu E_2

Servicing levels of assembly	Servicing structure of assembly E_2				
	e_1	e_2	e_3	e_4	e_5
1	⊗	⊗	⊗	⊗	⊗
2	⊗	⊗	⊗	⊗	⊗
3	⊗	$e_{3,2}$	⊗	⊗	⊗
4	$e_{4,1}$	⊗	⊗	⊗	⊗
5	⊗	⊗	$e_{5,3}$	⊗	⊗

On the further state of the listing (development) of the set of the object's operational information, a classification (grouping) of elements [6, 7] was conducted in order to distinguished classes (groups) of operational elements. With the use of the manner of classification of operational elements as presented in the article, the object's functional elements were grouped into operational classes. The results obtained are presented in Table 4.

Table 4. Classes of operational elements of assembly E_2
Tabela 4. Klasy elementów obsługowych zespołu E_2

Class of element	Subassembly of the assembly E_2				
	e_1	e_2	e_3	e_4	e_5
I – electronic	$e_{4,1}$	-	-	-	-
II – mechatronic	-	$e_{3,2}$	-	-	-
III – electric	-	-	$e_{5,3}$	-	-

The set of preventative activities is shown in Table 5. It describes all servicing and maintaining activities, which will be assign to particular elements of servicing structure of the object using relations 13 and relation 14 in [7].

Table 5. The set of preventive activities
Tabela 5. Zbiór czynności obsługowych

The set of preventive activities to renovate of the servicing object	
Replacement with new element	Code of activity
repair	10
Regulation	9
Tuning	8
Regeneration	7
Renovation	6
Conservation	5
Lubrication	4
Cleaning	3
Control checking	2
Replacement with new element	1

The set of diagnostic information (Table 4 and Table 5) was determined based upon above relations (1, 2, 0) and the known table of object states [3, 7]. The results obtained are presented in Table 6.

Table 6. Set of servicing structure of assembly E_2
Tabela 6. Struktura czynności obsługowych w zespole E_2

Servicing levels	Servicing structure of assembly E_2				
	e_1	e_2	e_3	e_4	e_5
1	∅	∅	∅	∅	∅
2	∅	∅	∅	∅	∅
3	∅	$\{a_1\}e_{3,2}$	∅	∅	∅
4	$\{a_2\}e_{4,1}$	∅	∅	∅	∅
5	∅	∅	$\{a_3\}e_{5.3}$	∅	∅

Based on information from Table 5 and Table 6, the model of the servicing system for particular object was settled. This model is represented by the set of structural elements and the set of preventive activities in matrix form (see Table 5) [3, 7]. The results obtained are presented in Table 7.

Table 7. Structure of system servicing of assembly E_2
Tabela 7. Struktura systemu obsługiwania dla zespołu E_2

Structure of system of object sevicing	
Element of servicing structure of the object	Elements of preventive activities structure
$e_{3,2}$	{1,2,6,9}
$e_{4,1}$	{1,2,7,9}
$e_{5,3}$	{1,3,6,9}

The set of operational rules $\{R_r(e_{i,j})\}$ constitutes an important subset of the set of operational information, whose diagram was presented in [7]. The set of operational rules was compiled according to the algorithm presented in the article. For this purpose, the previously obtained results in the form of stage sets of operational information were used, which were put in Tables 5, 6 and 7. The results obtained are presented in Table 8 and in Fig. 6.

Table 8. The set of operational rules for assembly E_2
Tabela 8. Zbiór reguł obsługowych dla zespołu E_2

Element no. in E_2 assembly	Rules of operation
$e_{1,1}$	R_1: If $\varepsilon(e_{1,1})$ is $\{\otimes\}$ then $M(e_{1,1}) = M_E(e_{1,1})$
$e_{1,2}$	R_2: If $\varepsilon(e_{1,2})$ is $\{\otimes\}$ then $M(e_{1,2}) = M_E(e_{1,2})$
$e_{1,3}$	R_3: If $\varepsilon(e_{2,1})$ is $\{\otimes\}$ then $M(e_{1,3}) = M_E(e_{1,3})$
$e_{2,1}$	R_4: If $\varepsilon(e_{2,2})$ is $\{\otimes\}$ then $M(e_{2,1}) = M_E(e_{2,1})$
$e_{2,2}$	R_5: If $\varepsilon(e_{2,2})$ is $\{\otimes\}$ then $M(e_{2,2}) = M_E(e_{2,2})$
$e_{2,3}$	R_6: If $\varepsilon(e_{2,3})$ is $\{\otimes\}$ then $M(e_{2,3}) = M_E(e_{2,3})$
$e_{3,1}$	R_7: If $\varepsilon(e_{3,1})$ is $\{\otimes\}$ then $M(e_{3,1}) = M_E(e_{3,1})$
$e_{3,2}$	R_8: If $\varepsilon(e_{3,2})$ is $\{1\}$ then $M(e_{3,2}) \rightarrow \{1,2,6,9,\} = M_E(e_{3,2})$
$e_{3,3}$	R_9: If $\varepsilon(e_{3,3})$ is $\{\otimes\}$ then $M(e_{3,3}) = M_E(e_{3,3})$
$e_{3,4}$	R_{10}: If $\varepsilon(e_{3,4})$ is $\{1\}$ then $M(e_{3,4}) = M_E(e_{3,4})$
$e_{3,5}$	R_{11}: If $\varepsilon(e_{3,5})$ is $\{\otimes\}$ then $M(e_{3,5}) = M_E(e_{3,5})$
$e_{4,1}$	R_{12}: If $\varepsilon(e_{4,1})$ is $\{1\}$ then $M(e_{4,1}) \rightarrow \{1,2,7,9\} = M_E(e_{4,1})$
$e_{4,2}$	R_{13}: If $\varepsilon(e_{4,2})$ is $\{\otimes\}$ then $M(e_{4,2}) = M_E(e_{4,2})$
$e_{4,3}$	R_{14}: If $\varepsilon(e_{4,3})$ is $\{\otimes\}$ then $M(e_{4,3}) = M(e_{4,3})$
$e_{5,1}$	R_{15}: If $\varepsilon(e_{5,1})$ is $\{\otimes\}$ then $M(e_{5,1}) = M(e_{5,1})$
$e_{5,2}$	R_{16}: If $\varepsilon(e_{5,2})$ is $\{\otimes\}$ then $M(e_{5,2}) = M_E(e_{5,2})$
$e_{5,3}$	R_{17}: If $\varepsilon(e_{5,3})$ is $\{1\}$ then $M(e_{5,3}) \rightarrow \{1,3,6,9\} = M_E(e_{5,3})$

The effect of the method presented in the article is the determined set of service information, which was presented in the form of $\{M_E(e_{i,j})\}$. This specialist knowledge base (a set of maintenance information) constitutes the basis for the designing of a reliable system of the maintenance (prevention) of a technical object. The designing of a maintenance system consists in the determination of the structure of the maintenance system (Fig. 6), which is composed of the following: the object's maintenance elements, the prevention activities (depending of the state) selected by an expert, including the maintenance means for a given element $\{A(e_{i,j})\}$, and maintenance rules $\{R_r(e_{i,j})\}$.

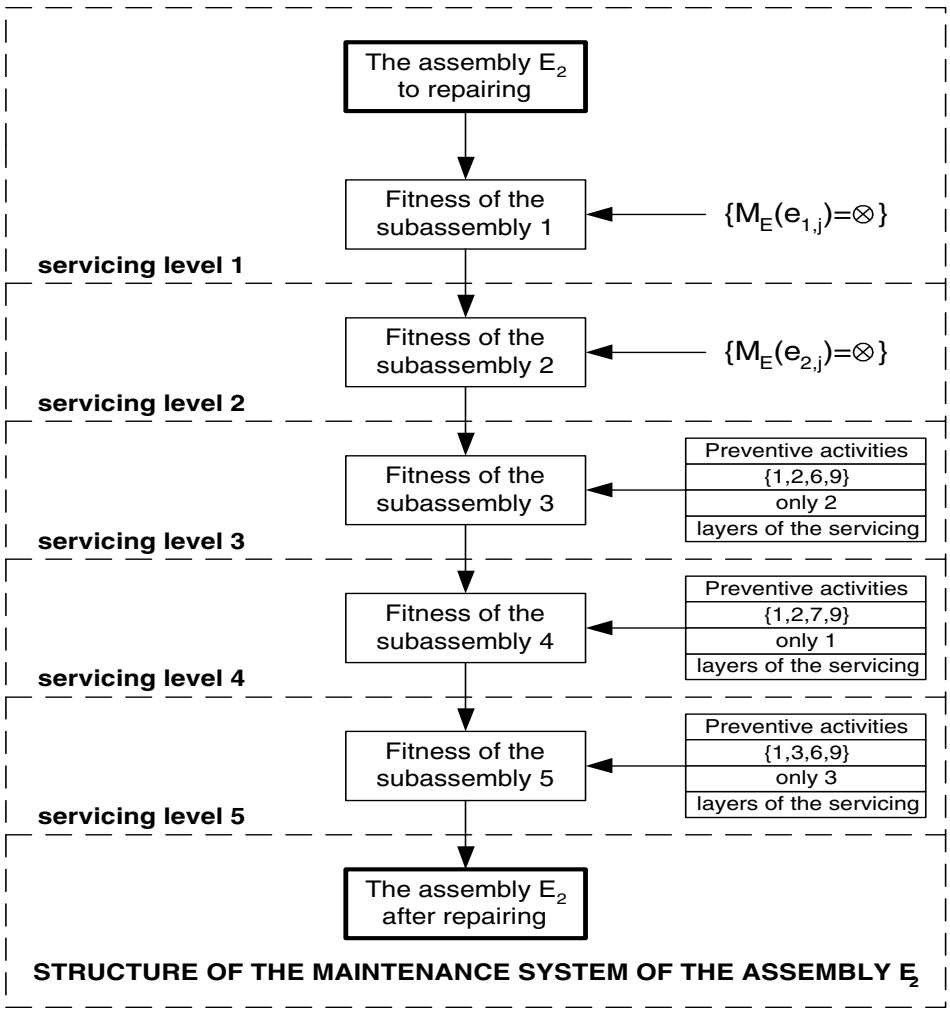

Fig. 6. The scheme of structure of the maintenance system of an assembly E_2
Rys. 6. Schemat struktury obsługowej zespołu E_2

The final form of the maintenance knowledge base was presented in the form of the information included in (Table 8) and Fig. 6. This table includes a set of maintenance rules for assembly E_2. Each rule included in this table determines explicitly which element of a given assembly of the object must be subject to regeneration, and what range of prevention activities (from the set of the activities) is to be performed on it. The execution of the determined set of maintenance rules will result in the regeneration of the whole element, assembly and the whole object. The technical object, once the maintenance has been performed, is subject to a control check-up (testing) of the state, and in the case of a negative result of the control, the object is once again referred to prevention.

The issues presented in the article of the creation (building) of a set of operating information concerns various fields of knowledge, including technical diagnostics, the theory of operation, information technology, expert systems, fuzzy sets, artificial neural networks, etc. Each of these fields is well and broadly worked out in the literature. It is the author's opinion that one can claim with full responsibility that even the basic problem, that is the use of diagnostic information obtained in the diagnosing process of a technical object in the designing and organisation of the operation process, is being constantly developed in various aspects (directions).

At present, the direction of the applications of neural networks, among others in the diagnostics of technical objects, is being intensively developed. However, new solutions and possibilities are constantly being sought; hence, the author's papers and studies are presented concerning a practical application of a trivalent evaluation (classification) of the object's states [4–8].

However, there is no full description in the literature of methods to develop ways and algorithms for the processing of diagnostic information obtained by diagnostic systems: an artificial neural network etc. to the form of an expert knowledge base of a maintenance system, presented in a computer programming language. A new problem, which in the author's opinion requires a solution, is the use of information developed in the trivalent evaluation of information states by the artificial neural network of information (knowledge) for the development of the method to control the prevention of technical objects, referred to in the literature as operation according to the object's state.

3. Conclusions

This paper presents of the method for the creation of an expert knowledge base. An important element of an expert knowledge base is information on the set of the elements of the object's maintenance structure, on the set of preventive activities to renovate the servicing object, on the set of preventive activities to renovate the servicing of technical objects with the required short shutdown time (aeroplanes, radiolocation systems, etc.). The basis of the method proposed is the

use of diagnostic information developed by a diagnostic system. The diagnostic information is developed in a diagnostic system of the recognition of the states of a reparable technical object with the use of an artificial neural network. The accepted method of diagnosis by a neural network consists in comparing the image of vectors of diagnostic signals with the images of their models. For this purpose, the technical object examined was subject to a diagnostic study. An important stage of the work is a functional and diagnostic analysis of the object. For this reason, the paper presents and describes the method of the division of the object's internal structure. As a result of this division, a set of basic elements and a set of diagnostic signals were determined.

References

[1] Będkowski L., Dąbrowski T. 2006: Podstawy eksploatacji cz. 2. Wyd. WAT, Warszawa, p. 187.
[2] Duer S.: The concept of assistant system for analogue class technical object servicing. Sixth International Conference On Unconventional Elektromechanical And Electrical System UEES'04. Alushta, The Crimea, Ukraine, 2004, pp. 687–690.
[3] Duer S.: System ekspertowy wykorzystujący trójwartościową informację diagnostyczną wspomagający obsługiwanie złożonego obiektu technicznego. Zagadnienia Eksploatacji Maszyn Z. 4(152) VOL. 42, 2007, pp. 195-208.
[4] Duer S.: An algorithm for the diagnosis of reparable technical objects utilizing artificial neural Network. Scientific Problems Of Machines Operation And Maintenance, Committee Of Machine Engineering Polish Academy Of Sciences. Vol. 43, No. 1(53) 2008, pp. 101-113.
[5] Duer S., Duer R., Duer P., Płocha I.: Measurement system for the diagnosis of analogue technical objects with the use of artificial neural networks. Academic Journals, Poznan University of Technology, s. Electrical Engineering, Published by Poznan University of Technology, No. (59) 2009, pp. 61-72.
[6] Duer S.: System ekspertowy, ze sztuczną siecią neuronową obsługujący zestaw stacji radiolokacyjnej. VII Krajowa Konferencja Inżynierii Wiedzy i Systemów Ekspertowych, Instytut Informatyki, Politechnika Wrocławska, 23–25 czerwca, Wrocław, 2009.
[7] Duer S.: Determination of an expert knowledge base for servicing of a repairable technical object. Scientific Problems Of Machines Operation And Maintenance, Committee Of Machine Engineering Polish Academy Of Sciences (2009) (in publishing).
[8] Duer S.: Artificial Neural Network-based technique for operation process control of a technical object. Defence Science Journal, Vol. 59, No. 3, May 2009, DESIDOC, pp. 01-09.
[9] Dhillon B.S.: Applied Reliability and Quality, Fundamentals, Methods and Procedures. Springer – Verlag London Limited, p. 186, 2006.
[10] Madan M. Gupta, Liang Jin and Noriyasu Homma: Static and Dynamic Neural Networks, From Fundamentals to Advanced Theory. John Walley End Sons, Inc, p. 718, 2003.
[11] Nakagawa T.: Maintenance Theory of Reliability. Springer – Verlag London Limited, p. 264, 2005.
[12] Nakagawa T. and Ito K.: Optimal inspection policies for a storage system with degradation at periodic tests. Math. Comput. Model. Vol. 31, pp. 191-195, 2000.
[13] Łosiński M., Duer S., Jaśkiewicz A., Drabarek J., Madej W.: Analiza efektywności procesu eksploatacji sprzętu przeciwlotniczego. WSOWOPL Nr 1035/94. Koszalin 1994, str. 120.
[14] Wiliams J. M. and Zipser D.: A learning Algorithm for Continually Running Fully Recurent Neural Networks. Neural Comput. vol. 1, pp. 270-280, 1989.
[15] Zurada I. M.: Introduction to Artificial Neural Systems. West Publishing Company, St. Paul, MN, p. 263, 1992.

Manuscript received by Editorial Board, May 25th, 2009

Tworzenie informacji obsługowej wspomagającej obsługiwanie obiektu technicznego wykorzystując trójwartościową informację diagnostyczną

S t r e s z c z e n i e

W pracy zaprezentowano metodę konstruowania struktury systemu obsługiwania naprawialnych obiektów technicznych. W proponowanej metodzie wykorzystano informację diagnostyczną ze sztucznej sieci neuronowej oraz wiedzę ekspertową. Zaprezentowano sposób realizacji opracowania obsługowego obiektu. Istotnym etapem w proponowanej metodzie zestawiania struktury systemu obsługiwania obiektu jest sposób przekształcania struktury wewnętrznej złożonego obiektu z jego elementami funkcjonalnymi do postaci struktury obsługowej obiektu. W artykule zawarto również analityczne podstawy wyznaczania informacji obsługowej (obsługowej wiedzy ekspertowej), organizującej system obsługiwania technicznego obiektu. Przedstawiono podstawy analityczne procesu odnawiania własności użytkowych obiektu obsługi.

SCIENTIFIC PROBLEMS
OF MACHINES OPERATION
AND MAINTENANCE
3 (159) 2009

ANDRZEJ KATUNIN*

Numerical study of delamination propagation in polymer-based laminates during quasi-static loading

Key words

Mode II delamination, polymer-based laminates, delamination propagation.

Słowa kluczowe

Delaminacja II rodzaju, laminaty polimerowe, propagacja delaminacji.

Summary

In this paper, the author presents the numerical investigation of the delamination propagation in polymer-based laminate rectangular plates subjected to bending with different configurations of initial delamination. Four cases of configurations of mode II initial delamination were investigated: End-Loaded Split, Cantilever Beam Enclosed Notch, End-Notched Flexure, and Centre-Notched Flexure. These configurations were chosen due to their most common occurrence in engineering practice. The author researched the possibility of delamination growth based on critical strain energy release rate and the dependence of its value from loading and initial delamination length. The author shows that classical methods of energy release rates calculation cannot be applied for multilayered composites in cases when the initial delamination occurs out of laminate mid-plane. The influence of the self-heating effect in steady-state to crack growth was also investigated. The energy release rates were obtained from numerical simulations using J-integral formulation. The character of the delamination propagation was modelled using the

* Department of Fundamentals of Machinery Design, Faculty of Mechanical Engineering, Silesian University of Technology, Konarskiego 18A, 44-100 Gliwice, Poland, e-mail: andrzej.katunin@polsl.pl

cohesive zone approach. Results of the simulation were presented as the damage function in dependence of loading and initial delamination length. The obtained results can be useful for the prediction of the delamination growth in quasi-static tests and for modelling the delamination propagation during dynamic excitation in fatigue tests.

1. Introduction

Wide applicability of polymer-based laminates determines the development of methods and techniques of their diagnosing and monitoring. Therefore, the behaviour of them in different operation states and conditions must be investigated. The problem becomes more complicated when these structures contain faults and imperfections.

One of the most crucial faults in polymer-based laminates is the delamination or the interlayer cracks. Delaminations can arise in significant phases of the exploitation of a laminate element and their initiation and propagation can be caused by different factors, like critical loads, high temperature, ageing of material, fatigue stiffness degradation, impacts or other sources of interlaminar stress concentrations. Moreover, delaminations can arise in manufacturing processes during lamination process, waterjet cutting, and other. Delaminations can cause stiffness losses of the laminate and its total failure. In fact, mechanisms of delamination propagation must be investigated for laminate structural performance evaluation.

It is well known that delaminations can initiate in three modes according to loading and boundary conditions. Various works were focused on the mode I delamination and it is already extensively studied [1,2]. The mode III delamination has special conditions of initiation, and in engineering practice it occurs rather rarely [2]. The largest and not fully investigated group of delamination is classified as mode II delaminations. It can be induced when the prenotched specimen is subjected to bending loads with different boundary conditions.

There are many theoretical and experimental studies concentrated on fracture mechanics of laminates. In such studies, the main parameter that must be identified is the delamination resistance. It can be obtained using significant approaches. The first approach consists in evaluation of the critical stress intensity factor $K_{II,c}$ for the initial delamination length a [2,3]. The most commonly used approach uses the critical energy release rate $G_{II,c}$ formulation, which was proposed by Irwin [4]. In many works there is a proposal of analytical evaluation of energy release rate based on simple beam theory and its further modifications [5]. Various computational techniques allow the determination of the energy release rate as the J-integral [6], virtual crack extension technique (VCET) or virtual crack closure technique (VCCT) [7]. These techniques found wide application in FEM simulations.

The author's works were concentrated on degradation degree evaluation [8] and fatigue processes in polymer-based laminates with additional phenomena.

The influence of self-heating on the laminate fatigue was investigated in [9,10]. In the present paper, the author focused on numerical simulation of delamination propagation when the prenotched specimens have different initial delamination length and when the delamination occurs between significant layers of the laminate. Four cases of mode II delamination were investigated: End-Loaded Split (ELS), Cantilever Beam Enclosed Notch (CBEN), End-Notched Flexure (ENF), and Centre-Notched Flexure (CNF). Results of numerical simulations of energy release rate values were presented as R-curves in Section 3. Then, the character of delamination propagation was investigated numerically based on the cohesive zone method. The delamination was presented as the damage function and dependencies of applied loading and initial crack length were studied.

2. Problem description and motivation

Definition and solution of problems of the fracture mechanics is based on equations of structural mechanics. Due to the consideration of polymer-based laminates, the material must be defined by viscoelastic constitutive relations. However, in many works, which were considered on fracture of polymer-based laminates (e.g. [5-7]), the author assumes the linear elastic delamination models. This assumption is true for quasi-static loading only.

In the present paper, the multidirectional CFRP laminate rectangular plate was taken into consideration. The structural formula of the laminate, characteristic dimensions and material properties were given by (1) and Table 1 [8], where E_1 and E_2 are Young's moduli, G_{12} is the shear modulus, ν_{12} is the Poisson ratio, ρ is the density and L, b, h, h_0 are length, width, height of the plate and height of the layer respectively, whose structure is represented by:

$$[0/60/-60/-60/60/0]_{4S} \tag{1}$$

Table 1. Material properties and characteristic dimensions of the plate
Tabela 1. Stałe materiałowe i charakterystyczne wymiary płyty

E_1 [GPa]	E_2 [GPa]	G_{12} [GPa]	ν_{12} [-]	ρ [kg/m^3]
38.283	10.141	3.533	0.366	1794
L [m]	B [m]	h [m]	h_0 [m]	
0.25	0.025	0.00528	0.00022	

2.1. Theoretical background

As it was noticed before, four mode II delamination configurations were chosen for the analysis: ELS, CBEN, ENF and CNF. These configurations are presented in Fig. 1.

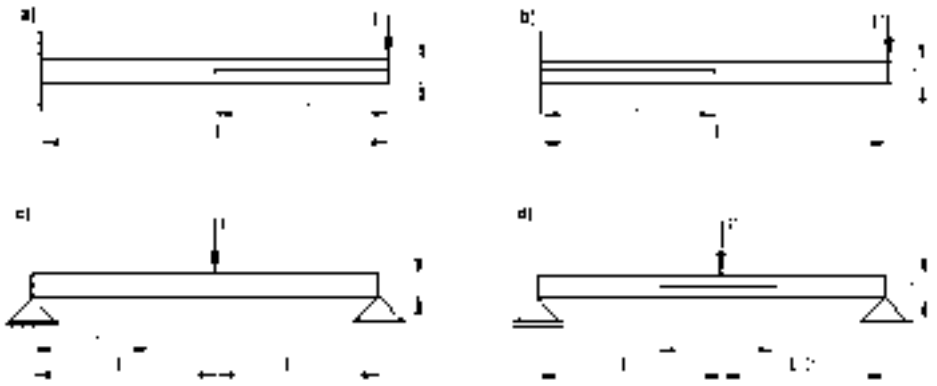

Fig. 1. Configurations of delamination, a) ELS, b) CBEN, c) ENF, d) CNF
Rys. 1. Konfiguracje delaminacji, a) ELS, b) CBEN, c) ENF, d) CNF

The presented configurations were based on typical experimental tests of delamination, which allow to determine delamination resistance given by critical stress intensity factors $K_{II,c}$ or critical energy release rates $G_{II,c}$, whereas there is the relation between the latter parameters. According to corrected beam theory $G_{II,c}$ can be presented by (2) for the investigated cases with respect to Fig. 1.

$$\begin{aligned} &\text{a), b)} \quad G_{II,c} = \frac{9P^2a^2}{4b^3E_1h^3}, \\ &\text{c), d)} \quad G_{II,c} = \frac{9P^2a^2}{16b^3E_1h^3}, \end{aligned} \tag{2}$$

where P is the applied load and a is the initial delamination length. The relation between $G_{II,c}$ and $K_{II,c}$ can be presented as:

$$G_{II,c} = \frac{K_{II,c}^2}{E'}, \; E' = E_1 \text{ for plane stress and } E' = \frac{E_1}{1-\nu^2} \text{ for plane strain.} \tag{3}$$

It is known that there is the equality between energy release rate and J-integral value. Therefore, there is a possibility to substitute the evaluation of $G_{II,c}$ values by J_c values in further investigations. The J-integral can be defined mathematically as path-independent contour integral and can be useful for crack analysis [11]. Physically, it is the measure of dissipative energy during crack propagation, which can be presented as:

$$J = -\frac{\partial U}{\partial a}, \tag{4}$$

where U is the potential energy [2].

For evaluation of delamination propagation character the cohesive zone method was used. This method is based on constitutive relationship between stress values and relative displacements value. The effective traction t is introduced as a function of effective opening displacement δ and is characterised by the initial reversible response followed by an irreversible response as soon as the critical effective opening displacement δ_c has been reached. The irreversible part is characterised by increasing the damage function ranging from 0 (onset delamination) to 1 (full delamination) [11]. In this study the exponential function (5) was used:

$$t = G_{II,c} \frac{\delta}{2\delta_c} \exp\left(-\frac{\delta}{\delta_c}\right), \tag{5}$$

where $G_{II,c}$ is the energy release rate or so-called cohesive energy.

2.2. Motivation

In investigations of the delamination of rectangular plates, there are several constraints if the analytical approach was chosen. First of all, the presented relations (2) assume that the delamination growth is stable; however, in the investigated case, the delamination growth instabilities can occur as well. Moreover, in (2), only the longitudinal Young modulus was taken into consideration, but in case of multidirectional laminate mechanical characteristics must be determined by four independent parameters. Referring to this, the 3-dimentional numerical model was prepared for solving the problem using MSC.Marc/Mentat commercial software, which allows one to model the delamination more realistically.

3. Numerical evaluation of energy release rates

The numerical model of the rectangular plate consists of 24 elastic bodies according to (1), which was meshed using hexagonal 8-node elements. Material properties were the same as in Table 1. The delamination in investigated cases between particular layers was modelled as a contact deactivation in interesting areas. Then, the delamination front was modelled using the crack tip node path along the width of the plate for 3-dimensional formulation. Boundary conditions were defined for each investigated case and the loading force P was applied as quarter-sine function (6) for defining it as a cyclic loading:

$$P = P_0 \sin(0.5\pi t), \tag{6}$$

where P_0 = 10 [N] is the static load and t is time variable defined as quasi-static time step for the analyses. The analysis was defined as mechanical static problem and J-integral values were calculated. In obtained results the values of energy release rates were chosen as a maximal value along the delamination front. Due to nonlinear

distribution of energy release rates along the delamination front it is necessary to be sure that the delamination occurs. Results of critical energy release rates for the different initial delamination length were presented as R-curves in Fig. 2. The analyses were provided for the initial delamination with $H = 0.5$. Here and further A_0 is the non-dimensional initial delamination length, z denotes the distance from bottom surface of the laminate to the delaminated area and H is the non-dimensional thickness parameter:

$$A_0 = \frac{a_0}{L},\ H = \frac{z}{h}. \tag{7}$$

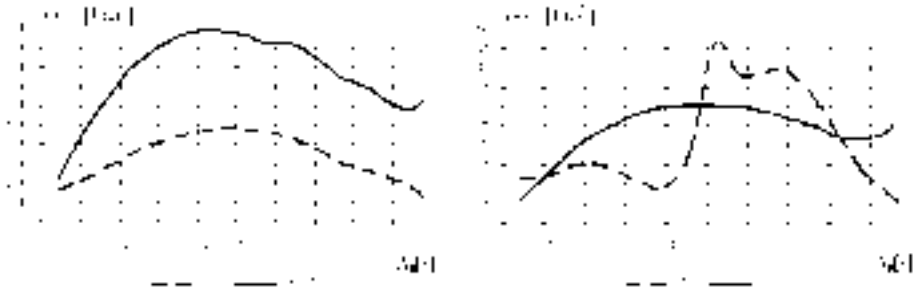

Fig. 2. R-curves for different initial delamination values
Rys. 2. Krzywe R dla różnych wartości delaminacji początkowej

According to the definition of delamination tests, which were taken into consideration and the modified beam theory, the initial delamination must be situated in the half thickness. In cases when the delamination occurs in different places, the values of energy release rates were not the same, therefore it was investigated in this study. R-curves were presented in Fig. 3 for ELS case.

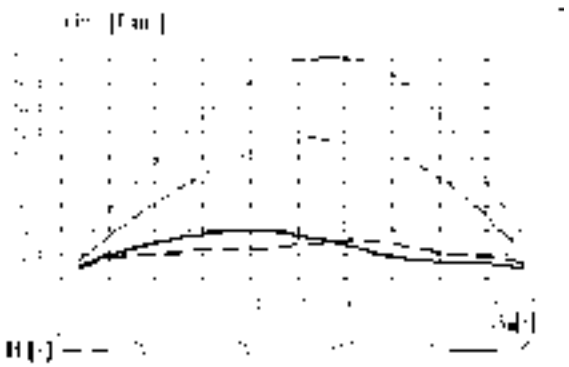

Fig. 3. R-curves for different initial delamination values and delaminated layers
Rys. 3. Krzywe R dla różnych wartości delaminacji początkowej i zdelaminowanych warstw

The *H* parameter values were chosen according to the orientation of pairs of layers between which the delamination occurs. Only five cases were chosen according to the symmetry of the laminate (see (1)). The investigated cases are presented in Table 2.

Table 2. Investigated cases of the delaminated layers
Tabela 2. Rozpartywane przypadki zdelaminowanych warstw

H [-]	0.5	0.75	0.875	0.917	0.958
Layers orientation [deg]	0/0	0/0	-60/-60	60/-60	0/60

For the investigated cases the dependence between applied loading *P* and displacements δ was also studied. Results were presented in Fig. 4.

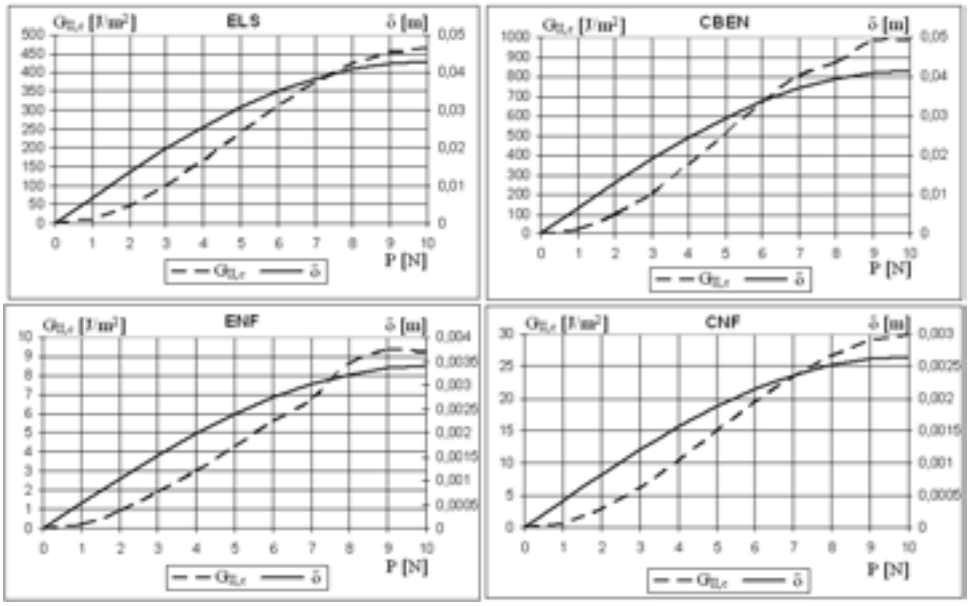

Fig. 4. Relations P-δ and P-$G_{II,c}$ for $A_0 = 0{,}4$
Rys. 4. Zależności P-δ oraz P-$G_{II,c}$ dla $A_0 = 0{,}4$

In the case of cyclic loading of the laminate, it reveals viscoelastic properties. During out-of-phase oscillations between stress and strain amplitudes, the mechanical energy is dissipated and transformed into the heat. According to low values of the thermal conductivity of the epoxy resin, the heat

accumulates in the structure and the self-heating effect is performed [12]. Due to the quasi-static formulation of the present problem, only the steady-state of the self-heating was taken into consideration. The numerical model was redefined for solving the coupled thermal-mechanical work and supplemented by the initial condition of the ambient temperature (293 K) and boundary condition of the temperature defined as:

$$\theta = Q\frac{\operatorname{sinc}\mu_m \operatorname{sinc}\gamma_n \cos\xi_m x \cos\xi_n y}{\left(1+\operatorname{sinc}2\mu_m\right)\left(1+\operatorname{sinc}2\gamma_n\right)\left(\xi_m^2+\xi_n^2\right)}+\theta_0, \tag{8}$$

where θ is the temperature distribution, Q is the dissipative heating, μ_m and γ_n are subsequent roots of the boundary-value characteristic equations, x and y are Cartesian coordinates, θ_0 is the ambient temperature and $\xi_m = \mu_m/L$ and $\xi_n = \gamma_n/b$.

Results of analyses show, that the influence of the self-heating effect in all the investigated cases on J-integral values is rather low, in all cases it did not exceed 0.1%, therefore it was neglected in calculations.

4. Evaluation of damage functions during delamination

For the evaluation of the character of the delamination growth the cohesive zone method was used. The numerical model was defined as in the previous section with additional changes. The cohesive zone was modelled using zero-thickness hexagonal 8-node interface elements, contact options between two interested layers were deactivated and the glue "second-to-first" contact was defined between the cohesive zone and each of contacted layers. Then, the geometrical properties were defined for the cohesive zone: They were defined as 3D interface with integration points located in Gauss points. Material properties for cohesive zone were defined as follows: the exponential cohesive model (5) was applied with critical opening displacement $\delta_c = 10^{-5}$ [m] and the cohesive energy was set up in order to obtain full delamination when the maximal force has been applied (Table 3.). For each of investigated cases, the $G_{II,c}$ value was different. The problem was defined as the mechanical static.

The obtained results were presented as the damage function D, which takes values "0" for healthy area and "1" for fully delaminated area. Results for the investigated cases are presented in Fig.5 as contour line plots, which presented dependence between the energy release rate, the delamination length and the applied force for $H = 0.5$ and $A_0 = 0.5$.

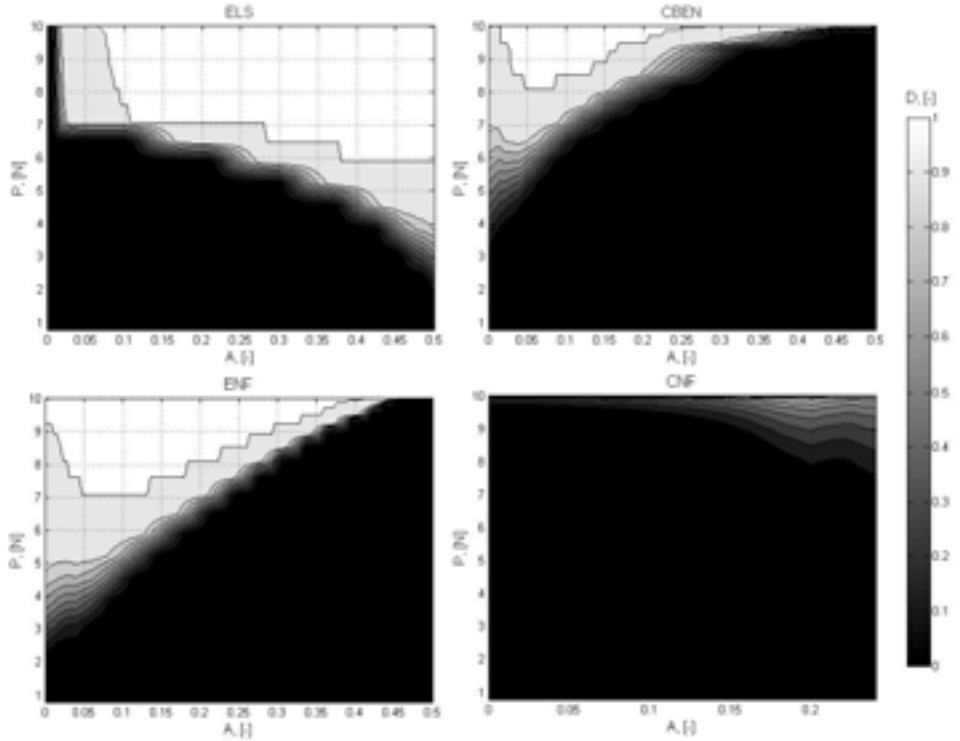

Fig. 5. Damage functions during delamination growth
Rys. 5. Funkcje uszkodzeń podczas przyrostu delaminacji

Table 3. Cohesive energy values of investigated cases
Tabela 3. Wartości energii dekohezji dla rozpatrywanych przypadków

Case identifier	ELS	CBEN	ENF	CNF
$G_{II,c}$ [J/m^2]	25	18	4.5	7.5

The next numerical research concerned the evaluation of the character of the delamination growth with different values of thickness of delamination occurring (Fig. 6) and different initial delamination values A_0 (Fig. 7). Results in Fig. 6 are presented for cases as in the previous section according to Table 2 for ELS models.

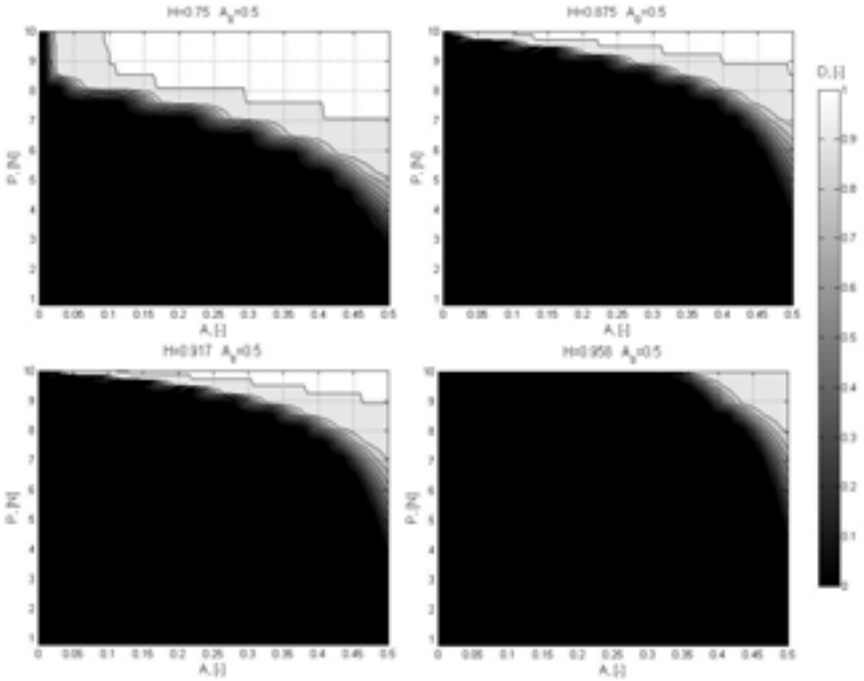

Fig. 6. Damage functions during delamination growth with different *H* parameter
Rys. 6. Funkcje uszkodzeń podczas przyrostu delaminacji z różnymi parametrami *H*

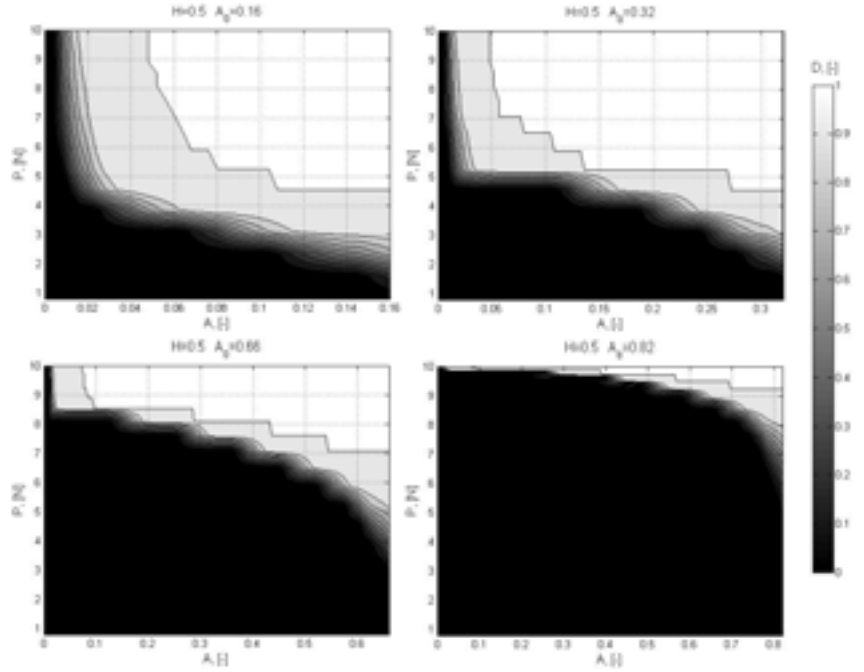

Fig. 7. Damage functions during delamination growth with different initial delamination
Rys. 7. Funkcje uszkodzeń podczas przyrostu delaminacji z różną delaminacją początkową

The delamination function is characterised by slow growth, when it attains near-one values. Figures presented below do not illustrate these small changes because of insufficient resolution of contour plots. Therefore, the fully delaminated regions in the given case can be presented as the delamination length in the function of the applied force. Such exemplary results are presented on Fig.8 for ELS configuration. The initial delamination A_0 in ELS, CBEN and ENF cases is equal to 0.5 and in CNF case is equal to 0.52.

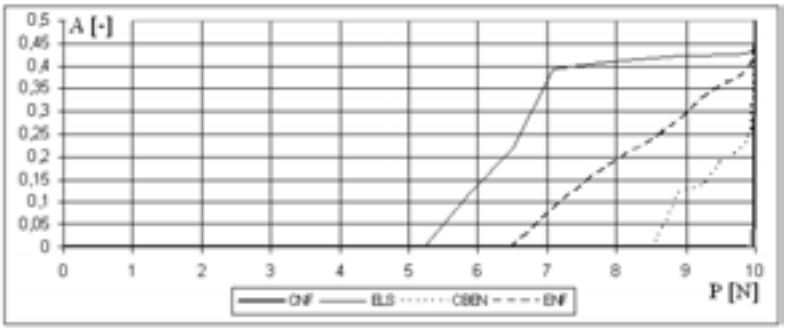

Fig. 8. Fully delaminated regions
Rys. 8. Całkowicie zdelaminowane obszary

5. Analysis of results

In the present work, the delamination process was studied numerically for four configurations of the initial delamination (Fig. 1). FE models were defined and calculated using MSC.Marc/Mentat commercial software. There are several directions of research presented in this work. We calculated the energy release rates on the delamination front in the dependence of the initial delamination length and in the dependence of the thickness, where the delamination occurs and presented results as R-curves (Fig. 2-3). Also, force-displacement and energy release rate-displacement dependencies were obtained (Fig. 4). Analyses were performed based on the J-integral formulation of the fracture. Then, the character of the delamination growth was studied using cohesive zone model formulation. Among others, the character of the delamination was studied for different values of the thickness where the delamination occurs (Fig. 6), and the initial delamination length (Fig. 7).

Analysing obtained R-curves for investigated cases (Fig. 2), one can notice that the delamination instability occurs at near half-length of the specimen, which is conformed with experimental results [2]. In case of ENF specimen (Fig. 2), there is a nonlinearity with higher order, which is caused by stress concentrations due to boundary conditions (Fig. 1). The next analyses for models with variable thickness parameter H show that, in cases when the delamination occurs out of mid-plane, the values of energy release rate are

different and characterised by a decreasing tendency, which can be explained by larger stresses due to increasing the distance from neutral plane of the laminate ($z \to h/2$). This can be asserted based on R-curves with $H = 0.5$ and $H = 0.75$ in Fig.3 while taking into consideration the identical layers orientation for both cases (Table 2). We also compared pairs of layers with different orientation (see Table 2); and based on results presented in Fig.3, we can affirm the great influence of the layers orientation on energy release rates. This phenomenon occurs due to the influence of the layers' orientation on layers' rigidity and can be obtained from classical theory of lamination. Analysing results of force-displacement dependencies for investigated cases (Fig. 4), we obtain quadratic curves which coincides with modified beam theory and relations (2). Such curves were used for determining the damage energy in experimental studies [2]. Dependencies between energy release rates and the applied force also show quadratic behaviour, which is justified by linear beam theory.

In case of cyclic loading of the polymer-based laminate, there are some energy losses according to the hysteretic behaviour of the laminate, due to the theory of linear thermoviscoelasticity. According to the quasi-static study presented in this work, only the steady-state self-heating was investigated. Results of numerical simulations show that, in all investigated cases, the difference between models with and without self-heating did not exceed 0.1%; therefore, the self-heating effect has not been taken into account and could be neglected in such simulations and tests.

The study concerned the investigation of the character of delamination propagation shows stable growth of the delamination in all the investigated cases (Fig. 5), which verifies previous simulations and obtained R-curves. Stepping of the applied force caused the observed non-linearity. As it can be noticed, the character of the delamination growth in investigated cases is similar. In Fig.6, the exemplary damage function distribution for ELS configuration with variable parameter H is presented. The results confirm previous investigations. It can be observed that, for $H = 0.5$ (Fig.5) and $H = 0.75$ (Fig.6), the character of the damage function distributions are the same, but values vary according to the distance from the neutral plane of the laminate. In cases with other values of H, the influence of layer orientations can also be observed. Simulations of the delamination with variable initial delamination (Fig. 7) show the nonlinear behaviour of the damage function, especially in first two cases. It can be noticed that, after exceeding some critical force value, the delamination becomes unstable.

6. Conclusions

Analysing obtained results in several numerical studies, we can conclude the impossibility of using analytical methods based on beam theory for solving

some specific problems of the delamination. The beam theory assumes that the material can be presented only by longitudinal Young's modulus, while in the case of non-isotropic structures, it behaves differently. Moreover, in standard tests for delamination evaluation, the initial delamination always is situated in mid-plane of the laminate. Therefore, the beam theory and dependencies (2) cannot be applied for evaluation of the energy release rates. Moreover, they cannot be used for a description of delamination behaviour, when it occurs in a plane other than the mid-plane (Fig. 6). Finally, the beam theory assumes growth stability during delamination process, but in many cases this assumption can give quite large differences.

The presented results are helpful for understanding the processes of the delamination propagation in multilayered structures. In further work, they will be used for modelling the high-cycle fatigue behaviour of such laminates. There are some additional effects that will be present in fatigue processes and constitute great scientific interest: hysteretic behaviour and thermal phenomena like non-steady self-heating and frictional heating in delaminated areas. The author's scientific group is going to carry out their research concerning these problems in the near future.

Acknowledgements

The author would like to thank for the financial support of the Polish Ministry of Science and Higher Education in research grant No. N N504 282137.

References

[1] Davies P., Blackman B.R.K., Brunner A.J., Standard test methods for delamination resistance of composite materials: current status, Applied Composite Materials, 5, pp. 345-364, 1998.

[2] Ochelski S., Experimental methods of constructional composite mechanics [in Polish], WNT, Warsaw 2004.

[3] Milašinovič D.D., Rheological-dynamical analogy: modeling of fatigue behavior, International Journal of Solids and Structures, 40, pp. 181-217, 2003.

[4] Irwin G.R., Fracture, in: Handbuch der Physik, vol. 6, Springer Verlag, Berlin 1958.

[5] Blackman B.R.K., Kinloch A.J., Paraschi M., The determination of the mode II adhesive fracture resistance, G_{IIc}, of structural adhesive joints: an effective crack length approach, Engineering Fracture Mechanics, 72, pp. 877-897, 2005.

[6] Zemčik R., Laš V., Numerical and experimental analyses of the delamination of cross-ply laminates, Materials and Technology, 4 (42), pp. 171-174, 2008.

[7] Muñoz J.J., Galvanetto U., Robinson P., On the numerical simulation of fatigue driven delamination with interface elements, International Journal of Fatigue, 28, pp. 1136-1146, 2006.

[8] Katunin A., Moczulski W., The conception of a methodology of degradation degree evaluation of laminates, Maintenance and Reliability, 1 (41), pp. 33-38, 2009.

[9] Katunin A., Moczulski W., Evaluation of self-activating temperature influence on crack initiation in GRP laminates, 80th Annual Meeting of the International Association of Applied Mechanics and Mathematics "GAMM 2009", CD Proceedings, Gdańsk 2009.
[10] Katunin A., Influence of self-heating temperature on the fatigue strength of a plate made of laminated polymeric composite, International Applied Mechanics, 45, 3, p. 342, 2009.
[11] Marc 2007r1. Volume A: Theory and user information, MSC.Software Corp., 2007.
[12] Katunin A., Self-heating effect in laminate plates during harmonic forced loading, Scientific Problems of Machine Operation and Maintenance, 44, 2(158), pp. 73-84, 2009.

Manuscript received by Editorial Board, February 02nd, 2010

Badania numeryczne propagacji delaminacji w polimerowych laminatach podczas obciążeń quasi-statycznych

S t r e s z c z e n i e

W niniejszej pracy autorzy prezentują badania numeryczne propagacji delaminacji w polimerowych laminatowych płytach prostokątnych poddanych zginaniu z różnymi konfiguracjami delaminacji wstępnej. Rozpatrzono cztery przypadki konfiguracji delaminacji wstępnej II rodzaju: End-Loaded Split, Cantilever Beam Enclosed Notch, End-Notched Flexure i Centre-Notched Flexure. Takie konfiguracje były wybrane ze względu na ich częste występowanie w praktyce inżynierskiej. Autorzy zbadali możliwość przyrostu delaminacji na podstawie krytycznego współczynnika uwalniania energii i zależności jego wartości od obciążenia i wstępnej długości delaminacji. Autorzy pokazali, że klasyczne metody wyznaczenia współczynników uwalniania energii nie mogą być zastosowane w przypadku wielowarstwowych kompozytów wtedy, gdy delaminacja inicjowana jest poza płaszczyzną środkową. Zbadano także wpływ efektu samorozgrzania w stanie ustalonym. Współczynniki uwalniania energii otrzymano z symulacji numerycznych z zastosowaniem sformułowania opartego na wyznaczeniu całki J. Charakter propagacji delaminacji był modelowany z wykorzystaniem modelu obszaru kohezji. Wyniki symulacji zaprezentowano w postaci funkcji zniszczenia w zależności od obciążenia i długości delaminacji wstępnej. Otrzymane wyniki mogą być wykorzystane przy predykcji przyrostu delaminacji w testach quasi-statycznych i przy modelowaniu propagacji delaminacji podczas wymuszenia dynamicznego i testów zmęczeniowych.

SCIENTIFIC PROBLEMS
OF MACHINES OPERATION
AND MAINTENANCE
3 (159) 2009

HENRYK TOMASZEK[*], SŁAWOMIR KLIMASZEWSKI[*],
MARIUSZ ZIEJA[*]

A probabilistic method of determining fatigue life of a structural component using the Paris formula and the probability density function of time of exceeding the boundary condition – an outline[**]

Key words

Fatigue life, density function, fatigue cracking.

Słowa kluczowe

Trwałość zmęczeniowa, funkcja gęstości, pękanie zmęczeniowe.

Summary

An attempt has been made to present a probabilistic method to determine fatigue life of an aeronautical structure's component by means of a density function of time a growing crack needs to reach the boundary condition. It has been assumed that in a component of a structure given consideration there is a small crack that grows due to fatigue load affecting it. After having reached the boundary value the component in question loses its usability. Time of the crack growth up to the boundary value is termed a fatigue life of the component. From the aspect of physics, the propagation of a crack within the component, if approached in a deterministic way, is

[*] Air Force Institute of Technology, ul. Księcia Bolesława 6, 01-494 Warszawa, tel.: +48 22 6851063, fax: +48 22 6851105. Poland.

[**] The article was presented on 35th International Scientific Congress on Powertrain and Transport Means – European KONES 2009.

described with the Paris's relationship for m = 2. To model the fatigue crack growth, a difference equation has been applied, from which the Fokker-Planck equation has been derived to be then followed with a density function of the growing crack. The in this way, the determined density function of the crack length has been applied to find density function of time of reaching the boundary condition. This function has been used in the present paper to determine the randomly approached fatigue life of a component of a structure.

1. Introduction

A matter under consideration is a method to determine fatigue life of a structural component of an aircraft. The following assumptions have been made:

- The component's health/maintenance status has been determined with one parameter only, i.e. the length of a crack therein. The actual value of the parameter has been denoted with *l*.
- Any change in the crack length may only occur in the course of the system/device being operated.
- In the case given, the consideration of the Paris formula takes the following form [1]:

$$\frac{dl}{dN_z} = CM_k^m \left(\sigma_{\max}\right)^m \pi^{\frac{m}{2}} l^{\frac{m}{2}} \tag{1}$$

where:

C, m – material constants,
N_z – a variable that denotes the number of the component-affecting load cycles due to the system's vibration,
M_k – coefficient of the finiteness of the component's dimensions at the crack location,
σ_{max} – maximum load defined with equation (2).

- The load upon the structure's component, with the system's vibration taken into account, is a destructive factor. Let us assume we have a component-affecting-load spectrum, with account taken of vibration. The spectrum allows for the determination of the following:
  - The total number of load cycles N_c in the course of one flight assumed a standard cycle.
  - Maximum loads within thresholds in the assumed spectrum amount to $\sigma_1^{\max}$, $\sigma_2^{\max}$, …, $\sigma_L^{\max}$ (the assumed number of thresholds in the spectrum is L).
  - The number of repetitions of specific threshold values of the loading during one flight (standard load) n_i, where:

$$N_c = \sum_{i=1}^{L} n_i \ .$$

- Maximum values of loads within the assumed thresholds are found in the following way:

$$\sigma_i^{\max} = \frac{\sigma_i^{\max} + \sigma_i^{\min}}{2} + \sigma_i^a, \tag{2}$$

where:

$\sigma_i^{\max}$ – maximum value of the cyclic load within the *i*-th threshold,

$\sigma_i^{\min}$ – minimum value of the cyclic load within the *i*-th threshold,

σ_i^a – the amplitude of the cyclic load within the *i*-th threshold.

- The following frequencies of the occurrence of loads correspond to values thereof within the thresholds $\sigma_1^{\max}$, $\sigma_2^{\max}$, …, $\sigma_L^{\max}$:

$$\frac{n_1}{N_c} = P_1,\ \frac{n_2}{N_c} = P_2,\ \ldots,\ \frac{n_L}{N_c} = P_L.$$

2. An outline of the method to determine probability density function of the component's crack length

Relationship (1) may be expressed against the flying time of the aircraft. Therefore, we assume that

$$N_z = \lambda t \tag{3}$$

where:

λ – the occurrence rate of load cycles upon the component,

t – flying time of the aircraft.

In the case under consideration

$$\lambda = \frac{1}{\Delta t},$$

where:

Δt – the average duration of the vibration-attributable fatigue-load cycle.

Relationship (1) against the flying time takes the following form:

$$\frac{dl}{dt} = \lambda C M_k^m \left(\sigma_{\max}\right)^m \pi^{\frac{m}{2}} l^{\frac{m}{2}} \tag{4}$$

Having applied the hitherto made assumptions, one can proceed to determine the relationship that describes the dynamics of the fatigue-crack growth, i.e. of the increase in its length.

Let $U_{l,t}$ denote the probability that at the time t (for the flying time equal to t) the crack reaches the length l. With the above-shown notation used, the dynamics of the crack length increase can be described with the following difference equation:

$$U_{l,t+\Delta t} = P_1 U_{l-\Delta l_1,t} + P_2 U_{l-\Delta l_2,t} + ... + P_L U_{l-\Delta l_L,t} \tag{5}$$

where:

P_i – probability that the load $\sigma_i^{\max}$ defined with equation (2) occurs, where $i = 1,2,3,.....,L$ and $P_1 + P_2 + P_3 + ... + P_L = 1$,

Δl_i – crack increment in time Δt for the load equal to $\sigma_i^{\max}$, where $i = 1,2,3,.....,L$. The increments are to be found on the grounds of dependence (4).

Equation (5) in function notation takes the following form:

$$u_{l,t+\Delta t} = \sum_{i=1}^{L} P_i u\left(l - \Delta l_i, t\right) \tag{6}$$

where:

$u(l,t)$ – the probability density function of the crack length, which depends on the flying time of the aircraft.

The difference equation (6) can be rearranged in the following partial differential equation of the Fokker-Planck type [3]:

$$\frac{\partial u(l,t)}{\partial t} = -\alpha(t)\frac{\partial u(l,t)}{\partial l} + \frac{1}{2}\beta(t)\frac{\partial^2 u(l,t)}{\partial l^2} \tag{7}$$

A particular solution of equation (7) is the crack-length density function of the following form:

$$u(l,t) = \frac{1}{\sqrt{2\pi A(t)}} e^{-\frac{(l-B(t))^2}{2A(t)}} \tag{8}$$

where:

$B(t)$ – an average crack length for the aircraft's flying time t,

$A(t)$ – crack-length variance for the aircraft's flying time t.

Equation (8) for the total flying time takes the form:

$$u(l,t_N)=\frac{1}{\sqrt{2\pi A(t_N)}}e^{-\frac{(l-B(t_N))^2}{2A(t_N)}} \tag{9}$$

where:

$t_N=\sum_{i=1}^{N}t_i$,

N – the number of flights by the aircraft,

t_i – duration of the i-th flight.

Coefficients $B(t_N)$ and $A(t_N)$ for the material constant m = 2 are solutions of the integrals [3]:

$$B(t_N)=\int_0^t \alpha(t_N)dt=l_0\left(e^{\lambda\overline{C_2}t_N}-1\right) \tag{11}$$

$$A(t_N)=\int_0^t \beta(t_N)dt=\frac{1}{2}l_0^2\overline{C_2}\omega\left(e^{2\lambda\overline{C_2}t_N}-1\right) \tag{12}$$

where:

$$\overline{C_2}=C_2\mathrm{E}[(\sigma^{\max})^2],$$

$$C_2=CM_k^2\pi,$$

$$\omega=\frac{\mathrm{E}[(\sigma^{\max})^4]}{(\mathrm{E}[(\sigma^{\max})^2])^2}.$$

3. An outline of the method to find the probability density function of the time of exceeding the permissible (boundary) value by the length of the crack in the component, for m = 2

Using the density function of the crack length (9), dependant on the flying time of the aircraft, one can determine the probability that the actual length of the crack in the aircraft structure's component exceeds the permissible value within the time interval (0, t_N). The relationship is as follows:

$$Q(t_N, l_d) = \int_{l_d}^{\infty} u(l, t_N) dl \tag{13}$$

where:

l_d – the permissible value of the crack length as determined for some assumed risk of failure to the structural component.

The probability density function of the flying time up to the moment the crack exceeds the permissible value will be determined by the following equation:

$$f(t) = \frac{\partial}{\partial t_N} Q(t_N, l_d) \tag{14}$$

From equation (14) the following is derived:

$$f(t_N, l_d) = u(l_d, t_N)[l_0 \lambda \overline{C_2} e^{\lambda \overline{C_2} t_N} + \frac{(l_d - l_0(e^{\lambda \overline{C_2} t_N} - 1)\lambda \overline{C_2} e^{2\lambda \overline{C_2} t_N})}{(e^{2\lambda \overline{C_2} t_N} - 1)}] \tag{15}$$

where:

$$u(l_d, t_N) = \frac{1}{\sqrt{2\pi(\frac{1}{2} l_0^2 \overline{C_2} \omega(e^{2\lambda \overline{C_2} t_N} - 1))}} e^{-\frac{(l_d - l_0(e^{\lambda \overline{C_2} t_N} - 1))^2}{l_0^2 \overline{C_2} \omega(e^{2\lambda \overline{C_2} t_N} - 1)}} \tag{16}$$

The way of finding the probability density function of time of exceeding the permissible condition (15) is given in [2], pp. 87 – 90.

4. An outline of the way of estimating the life of the aircraft structure's component, with the probability density function of the time of exceeding the permissible condition for m = 2

The formula for the reliability of the aircraft structure's component can be written in the following form:

$$R(t_N) = 1 - \int_0^t f(t_N, l_d) dt \tag{17}$$

where, the probability density function $f(t_N, l_d)$ is given by formula (15).

The unreliability of the component is then defined by the following equation:

$$Q(t_N)=\int_0^t U(l_d,t_N)[l_0\lambda\overline{C_2}e^{\lambda\overline{C_2}t_N}+\frac{(l_d-l_0(e^{\lambda\overline{C_2}t_N}-1)\lambda\overline{C_2}e^{2\lambda\overline{C_2}t_N})}{(e^{2\lambda\overline{C_2}t_N}-1)}]dt \tag{18}$$

where, $u(l_d, t_N)$ is determined with formula (16).

Integral (18) should be re-arranged in the simpler form and the problem reduced to solving the indefinite integral

$$\int f(t_N,l_d)dt \tag{19}$$

The following change has been made in the integrand:

$$\underbrace{\frac{(l_d-l_0(e^{\lambda\overline{C_2}t_N}-1))^2}{l_0^2\overline{C_2}\omega(e^{2\lambda\overline{C_2}t_N}-1)}}_{\text{"1"}}=\underbrace{\frac{(l_0(e^{\lambda\overline{C_2}t_N}-1)-l_d)^2}{l_0^2\overline{C_2}\omega(e^{2\lambda\overline{C_2}t_N}-1)}}_{\text{"2"}} \tag{20}$$

Expression “1” is to be replaced with expression “2”, and expression “2” is denoted with z:

$$\frac{(l_0(e^{\lambda\overline{C_2}t_N}-1)-l_d)^2}{l_0^2\overline{C_2}\omega(e^{2\lambda\overline{C_2}t_N}-1)}=z\,.$$

Hence,

$$\frac{dz}{dt}=\frac{2[l_0(e^{\lambda\overline{C_2}t_N}-1)-l_d]l_0\lambda\overline{C_2}e^{\lambda\overline{C_2}t_N}[l_0^2\overline{C_2}\omega(e^{2\lambda\overline{C_2}t_N}-1)]-[l_0(e^{\lambda\overline{C_2}t_N}-1)-l_d]^2 2\lambda l_0^2\overline{C_2}^2\omega e^{2\lambda\overline{C_2}t_N}}{l_0^4\overline{C_2}^2\omega^2(e^{2\lambda\overline{C_2}t_N}-1)^2}$$

$$\frac{dz}{dt}=\frac{2l_0^3\overline{C_2}^2\lambda\omega[l_0(e^{\lambda\overline{C_2}t_N}-1)-l_d](e^{2\lambda\overline{C_2}t_N}-1)e^{\lambda\overline{C_2}t_N}-2\lambda l_0^2\overline{C_2}^2\omega[l_0(e^{\lambda\overline{C_2}t_N}-1)-l_d]^2e^{2\lambda\overline{C_2}t_N}}{l_0^4\overline{C_2}^2\omega^2(e^{2\lambda\overline{C_2}t_N}-1)^2}$$

$$\frac{dz}{dt}=\frac{2l_0\lambda[l_0(e^{\lambda\overline{C_2}t_N}-1)-l_d](e^{2\lambda\overline{C_2}t_N}-1)e^{\lambda\overline{C_2}t_N}-2\lambda[l_0(e^{\lambda\overline{C_2}t_N}-1)-l_d]^2e^{2\lambda\overline{C_2}t_N}}{l_0^2\omega\,(e^{2\lambda\overline{C_2}t_N}-1)^2}$$

$$dt = \frac{l_0^2 \omega\ (e^{2\lambda \overline{C_2} t_N} - 1)^2}{2l_0 \lambda [l_0 (e^{\lambda \overline{C_2} t_N} - 1) - l_d](e^{2\lambda \overline{C_2} t_N} - 1) e^{\lambda \overline{C_2} t_N} - 2\lambda [l_0 (e^{\lambda \overline{C_2} t_N} - 1) - l_d]^2 e^{2\lambda \overline{C_2} t_N}} dz .$$

Then, the substitution has been made in the indefinite integral:

$$\int l_0 \lambda \overline{C_2} e^{\lambda \overline{C_2} t_N} + \frac{[(l_d - l_0 (e^{\lambda \overline{C_2} t_N} - 1)] \lambda \overline{C_2} e^{2\lambda \overline{C_2} t_N}}{(e^{2\lambda \overline{C_2} t_N} - 1)} \times$$

$$\times [\frac{l_0^2 \omega\ (e^{2\lambda \overline{C_2} t_N} - 1)^2}{2l_0 \lambda [l_0 (e^{\lambda \overline{C_2} t_N} - 1) - l_d](e^{2\lambda \overline{C_2} t_N} - 1) e^{\lambda \overline{C_2} t_N} - 2\lambda [l_0 (e^{\lambda \overline{C_2} t_N} - 1) - l_d]^2 e^{2\lambda \overline{C_2} t_N}}] \times$$

$$\times \frac{1}{\sqrt{\pi l_0^2 \overline{C_2} \omega (e^{2\lambda \overline{C_2} t_N} - 1))}} e^{-z} dz \qquad (21)$$

Hence,

$$\frac{1}{2\sqrt{\pi}} \int [l_0 \lambda e^{\lambda \overline{C_2} t_N} (e^{2\lambda \overline{C_2} t_N} - 1) + (l_d - l_0 (e^{\lambda \overline{C_2} t_N} - 1)] \lambda e^{2\lambda \overline{C_2} t_N}] \times$$

$$\times [\frac{1}{l_0 \lambda (e^{2\lambda \overline{C_2} t_N} - 1) e^{\lambda \overline{C_2} t_N} + [\lambda (l_d - l_0 (e^{\lambda \overline{C_2} t_N} - 1) e^{2\lambda \overline{C_2} t_N}]}] \frac{1}{\sqrt{z}} e^{-z} dz .$$

Therefore, the following is arrived at:

$$\frac{1}{2\sqrt{\pi}} \int \frac{1}{\sqrt{z}} e^{-z} dz .$$

After the rearrangements indefinite integral (21) takes the following form:

$$\frac{1}{2\sqrt{\pi}} \int \frac{1}{\sqrt{z}} e^{-z} dz \qquad (22)$$

Then, the second substitution has to be made in the integral (22), which should take the following form:

$$\sqrt{z} = w$$

$$\frac{dw}{dz} = \frac{1}{2\sqrt{z}}$$

$$\frac{dz}{dw} = 2w$$

$$dz = 2wdw \tag{23}$$

Dependence (23) is inserted in integral (22). Hence, the following is arrived at:

$$\frac{1}{2\sqrt{\pi}} \int \frac{1}{w} e^{-w^2} 2wdw = \frac{1}{\sqrt{\pi}} \int e^{-w^2} dw \tag{24}$$

One more substitution:

$$w^2 = \frac{y^2}{2}$$

$$2wdw = ydy$$

$$dw = \frac{y}{2w} dy$$

$$dw = \frac{dy}{\sqrt{2}}. \tag{25}$$

Hence, after inserting (25) in (24) the following integral is effected:

$$\frac{1}{\sqrt{2\pi}} \int e^{-\frac{y^2}{2}} dy \tag{26}$$

where, y takes the value determined with dependence (27), since

$$\frac{y^2}{2} = w^2; \qquad w = \sqrt{z}; \qquad z = \frac{(l_0(e^{\lambda \overline{C_2} t_N} - 1) - l_d)^2}{l_0^2 \overline{C_2} \omega (e^{2\lambda \overline{C_2} t_N} - 1)}$$

$$w = \sqrt{\frac{(l_0(e^{\lambda \overline{C_2} t_N} - 1) - l_d)^2}{l_0^2 \overline{C_2} \omega (e^{2\lambda \overline{C_2} t_N} - 1)}}$$

$$w = \frac{(l_0(e^{\lambda \overline{C_2} t_N} - 1) - l_d)}{\sqrt{l_0^2 \overline{C_2} \omega (e^{2\lambda \overline{C_2} t_N} - 1)}}$$

$$w^2 = \frac{y^2}{2}$$

$$y^2 = 2w^2$$

$$y = \sqrt{2w^2}$$

$$y = w\sqrt{2} = \sqrt{2}\frac{(l_0(e^{\lambda\overline{C_2}t_N} - 1) - l_d)}{\sqrt{l_0^2\overline{C_2}\omega(e^{2\lambda\overline{C_2}t_N} - 1)}} \tag{27}$$

Having inserted the results gained in equation (17) and remembering about a suitable notation of the limits of integration, the following dependence for the reliability is arrived at:

$$R(t) = 1 - \frac{1}{\sqrt{2\pi}}\int_{-\infty}^{y(t)} e^{-\frac{y^2}{2}} dy \tag{28}$$

where, equation (27) should be substituted for the upper limit of the integral *y(t)*.

The cumulative distribution function for the standard Gaussian (normal) distribution takes the following form:

$$\Phi(x) = \frac{1}{\sqrt{2\pi}}\int_{-\infty}^{x} e^{-\frac{y^2}{2}} dy\,.$$

With the above-shown dependence taken into account, the formula for the reliability of the structure's component is expressed with the following equation:

$$R(t_N) = 1 - \Phi(\sqrt{2}\frac{(l_0(e^{\lambda\overline{C_2}t_N} - 1) - l_d)}{\sqrt{l_0^2\overline{C_2}\omega(e^{2\lambda\overline{C_2}t_N} - 1)}})\,. \tag{29}$$

Hence, reliability of the structure's component will be determined with the following dependence:

$$Q(t_N) = \frac{1}{\sqrt{2\pi}}\int_{-\infty}^{\sqrt{2}\frac{[l_0(e^{\lambda\overline{C_2}t_N} - 1) - l_d]}{\sqrt{l_0^2\overline{C_2}\omega(e^{2\lambda\overline{C_2}t_N} - 1)}}} e^{-\frac{y^2}{2}} dy\,. \tag{30}$$

Having found (assumed) the level of risk of a failure to the structure's component, i.e. the level of exceeding the permissible value of the length of a crack in this component, we get the following:

$$Q(t_N) = Q^* \tag{31}$$

Hence,

$$Q^* = \frac{1}{\sqrt{2\pi}} \int_{-\infty}^{\vartheta} e^{-\frac{y^2}{2}} dy \tag{32}$$

For the assumed value of Q^*, the value of the upper limit of the integral (for which the integral on the right side of equation (32) takes value Q^*) is to be found in the standard Gaussian distribution tables.

Hence, the following dependence is arrived at:

$$\vartheta = \sqrt{2} \frac{(l_0(e^{\lambda \overline{C_2} t_N} - 1) - l_d)}{\sqrt{l_0^2 \overline{C_2} \omega (e^{2\lambda \overline{C_2} t_N} - 1)}} \tag{33}$$

$$\frac{\vartheta}{\sqrt{2}} = \frac{(l_0(e^{\lambda \overline{C_2} t_N} - 1) - l_d)}{\sqrt{l_0^2 \overline{C_2} \omega (e^{2\lambda \overline{C_2} t_N} - 1)}}$$

We assume that

$$\frac{\vartheta}{\sqrt{2}} = \vartheta^* .$$

Hence,

$$\vartheta^* = \frac{(l_0(e^{\lambda \overline{C_2} t_N} - 1) - l_d)}{\sqrt{l_0^2 \overline{C_2} \omega (e^{2\lambda \overline{C_2} t_N} - 1)}} \tag{34}$$

From (34) we can find time t_N^*, for which equality relation (34) takes place. Time t_N^* will be the searched life of the structure's component, i.e. it will be the aircraft's flying time for the assumed risk of exceeding the permissible value of the crack length. We assume that

$$e^{\lambda \overline{C_2} t_N} = x \tag{35}$$

Hence,

$$\vartheta^* = \frac{(l_0(x-1) - l_d)}{\sqrt{l_0^2 \overline{C_2} \omega (x^2 - 1)}} \tag{36}$$

From (36) we can find x. With some specific value of x gained from dependence (35), we can find t_N^*:

$$e^{\lambda \overline{C_2} t_N} = x$$

$$\lambda \overline{C_2} t_N = \ln x$$

$$t_N^* = \frac{\ln x}{\lambda \overline{C_2}} \tag{37}$$

Formula (37) determines the fatigue life of the aircraft structure's component t_N^* for the assumed risk of exceeding the boundary condition Q^*.

5. Final remarks

This paper has presented an outline of a method to determine the fatigue life of an aircraft structure's component. What provokes a fatigue process is a random load in the form of load spectrum. It should be emphasised that it is possible to find the fatigue life of a component using a more complex load spectrum. It has been assumed in the paper that the sequence of load cycles, as far as values thereof are concerned, has no effect upon the crack growth rate. All the dependencies arrived at enable specific calculations, if we have values of material constants and data on the load spectrum.

The present paper has been prepared for the case there is coefficient m = 2 in the Paris formula. With the in the paper presented scheme, one can find the fatigue life of the structure's component for the case m ≠ 2.

References

[1] Smirnov N.N, Ickovicz A.A., Obsłuzivanije i remont aviacjonnej techniki po sostojaniju, Transport, 1980.
[2] Tomaszek H., Żurek J., Jasztal M., Prognozowanie uszkodzeń zagrażających bezpieczeństwu lotów statków powietrznych, Radom, NITE, 2008.
[3] Kałmucki W.S., Prognozirowanije resursov detali maszin i elementov konstrukcji, Kisziniev,1989.
[4] Tomaszek H., Ważny M., Zarys metody oceny trwałości na zużycie powierzchniowe elementów konstrukcji z wykorzystaniem rozkładu czasu przekraczania stanu granicznego (dopuszczalnego), ZEM 3(155)/2008.

Manuscript received by Editorial Board, December 29th, 2009

Zarys probabilistycznej metody wyznaczania trwałości zmęczeniowej elementu konstrukcji z wykorzystaniem wzoru Parisa i funkcji gęstości czasu przekraczania stanu granicznego*

S t r e s z c z e n i e

W artykule podjęto próbę przedstawienia probabilistycznej metody wyznaczenia trwałości zmęczeniowej elementu konstrukcji lotniczej korzystając z funkcji gęstości czasu osiągania stanu granicznego przez narastające pęknięcie. Przyjęto, że w elemencie konstrukcji jest małe pęknięcie, które wzrasta pod wpływem obciążenia zmęczeniowego. Po osiągnięciu wartości granicznej element konstrukcyjny traci przydatność do użycia. Czas narastania pęknięcia do wartości granicznej określony jest jako trwałość zmęczeniowa elementu. Od strony fizycznej narastanie pęknięcia elementu w ujęciu deterministycznym określane jest przez zależność Parisa dla m = 2. Do modelowania wzrostu pęknięcia zmęczeniowego wykorzystano równanie różnicowe, z którego otrzymano równanie Fokkera-Plancka, a następnie funkcję gęstości narastającego pęknięcia. Określoną w ten sposób funkcję gęstości długości pęknięcia wykorzystano do wyznaczenia funkcji gęstości czasu osiągania stanu granicznego. Ta funkcja w niniejszej pracy posłużyła do określenia trwałości zmęczeniowej elementu konstrukcji w ujęciu losowym.

* Niniejszy artykuł został zaprezentowany na konferencji „35th International Scientific Congress on Powertrain and Transport Means – European KONES 2009.

SCIENTIFIC PROBLEMS
OF MACHINES OPERATION
AND MAINTENANCE
3 (159) 2009

TOMASZEK HENRYK[*], ŻUREK JÓZEF[*], STĘPIEŃ SŁAWOMIR[**]

The outline of the method for determining the fatigue limit of an element of aeronautical construction with the use of the density function of time of the limit state exceedance

Key words

Fatigue crack, limit state (admissible state), density function, fatigue limit.

Słowa kluczowe

Pękanie zmęczeniowe, stan graniczny (dopuszczalny), funkcja gęstości, trwałość zmęczeniowa.

Summary

The paper [3] presents the outline of a probabilistic method for determining the fatigue limit of an element of construction with the use of the Paris formula for $m = 2$ and the density function of time of the limit state exceedance. This article presents also the method for determining the fatigue limit of an element of construction for the density function of time of the time limit exceedance and the Paris formula for $m \neq 2$.

The Fokker-Planc equation and difference equations were used to model the fatigue crack. The solution of the Fokker-Planc equation is the unknown density function of the crack length, which was later used to find the density function of time of the limit state exceedance of the crack.

The latter density function was used to estimate the fatigue limit.

[*] Air Force Institute of Technology, ul. Księcia Bolesława 6, 01-494 Warszawa, Polnand, tel. (0-22) 6851956, faks (0-22) 836 44 71.

[**] Military University of Technology WAT, ul. Kaliskiego 2, 00-908 Warszawa, Poland, tel. (0-22) 6837789, faks (0-22) 683 93 18.

1. Introduction

The following conditions are assumed:

1) The destructive factor is the loading of the element including oscillations of the system.
2) We assume that we have the spectrum of the element loading (including oscillations) which enables determination of:
   - the total number of cycles of the loading N_c during one flight (cycle),
   - max. threshold loadings in the assumed spectrum are: $\sigma_1^{\max}, \sigma_2^{\max}, ..., \sigma_L^{\max}$ (it is assumed that there are L thresholds in the spectrum),
   - the number of reps of particular values of threshold loadings in one flight (cycle) is n_i, where: $N_c = \sum_{i=1}^{L} n_i$
3) Max. values of the assumed threshold loadings are determined in the following way:

$$\sigma_i^{\max} = \frac{\sigma_i^{\max} + \sigma_i^{\min}}{2} + \sigma_i^a \tag{1}$$

where: $\sigma_i^{\max}$ - max. value of cyclic loading at i-threshold;

$\sigma_i^{\min}$ - min. value of cyclic loading at i-threshold;

σ_i^a - amplitude of cyclic loading at i-threshold, $i = 1,2,...,L.$

4) Max. values of loading at the assumed thresholds during one cycle, i.e. during one flight or during one hour of flight are determined in the following way: Subsequent values of loading at threshold $\sigma_1^{\max}$, $\sigma_2^{\max}$, ... , $\sigma_L^{\max}$ correspond to the following frequencies of their occurrence $\frac{n_1}{N_c} = P_1$, $\frac{n_2}{N_c} = P_2$, ..., $\frac{n_L}{N_c} = P_L$.

Thus, we obtain the probabilistic characteristics of the loading of a particular element of construction in each flight or assumed working cycle of an aircraft.

5) It is assumed that, in respect of the working cycle, the occurrence of lower loading after the higher one and vice versa will not (concerning the effects) require additional changes.
6) It is assumed that the speed of fatigue crack growth follows the Paris equation:

$$\frac{dl}{d N_z} = C(\Delta K)^m \tag{2}$$

where: ΔK – the range of changes of values of stress intensity factor;
C, m – material constants;
l – crack length;
N_z – a variable – the number of loading cycles.

Let us consider the following equation:

$$N_z = \lambda t \tag{3}$$

where: λ – the intensity of occurrence of loading cycles,
t – the flying time of an aircraft.

In our case $\lambda = \frac{1}{\Delta t}$ where Δt is the duration time of fatigue load cycle. The equation (2) in the function of time has the following form:

$$\frac{dl}{d t} = \lambda C M_k^m (\sigma_{\max})^m \pi^{\frac{m}{2}} l^{\frac{m}{2}} \tag{4}$$

Using the above findings, we can now determine the equation describing the dynamics of fatigue crack growth. Let $U_{l,t}$ denote the probability that in the moment t (for the flying time equal to t) the length of crack will be l. We can describe the dynamics of crack length growth using the following difference equation:

$$U_{l,\,t+\Delta t} = P_1 U_{l-\Delta l_1,\,t} + P_2 U_{l-\Delta l_2,\,t} + \cdots + P_L U_{l-\Delta l_{L,\,t}} \tag{5}$$

where: P_i – the probability of the occurrence of stress in fatigue cycle; its value $\sigma_i^{\max}$ is described by equation (1) (i = 1, 2,..., L). These probabilities satisfy the following equation: $P_1 + P_2 + ... + P_L = 1$
Δl_i – crack growth in time Δt for stress value equal to $\sigma_i^{\max}$ (i = 1, 2,..., L). These growths can be determined from equations (1) and (4).

The difference equation (5) has the following meaning: The probability that for the flying time equal $t + \Delta t$, the crack will be l is equal to the sum of

probabilities that for the flying time equal to t , the crack was l - $\Delta l_{śr}$ and at the time interval $(t, t + \Delta t)$ it increased by value $\Delta l_{śr}$, where $\Delta l_{śr}$ is calculated from discrete values of loading in a cycle. The difference equation (5) has the following form in a functional notation:

$$u(l,\, t+\Delta t) = \sum_{i=1}^{L} P_i u\ (l - \Delta l_i,\, t) \tag{6}$$

where: $u(l,t)$ – the probability density function of crack length which is dependent on the flying time of an aircraft. We convert the equation (6) into partial differential equation. We obtain the following equation:

$$\frac{\partial u(l,t)}{\partial t} = -\alpha(t)\frac{\partial u(l,t)}{\partial l} + \frac{1}{2}\beta(t)\frac{\partial^2 u(l,t)}{\partial l^2} \tag{7}$$

The solution of the equation (7) is the density function of crack length in the following form:

$$u(l,t) = \frac{1}{\sqrt{2\pi\, A(t)}}\ e^{-\frac{(l-B(t))^2}{2A(t)}} \tag{8}$$

where: $B(t)$ – mean value of crack length for the flying time equal to t;
$A(t)$ – variance of crack length for the flying time equal to t.

2. Determination of the Flying Time Distribution up to the Moment when the Crack Reaches the Limit State (Admissible State) for the Coefficient m≠2

The density function of crack length has the following form:

$$u(l,t) = \frac{1}{\sqrt{2\pi\, A(t)}}\ e^{-\frac{(l-B(t))^2}{2A(t)}} \tag{9}$$

where: l – crack length,
t – the flying time of an aircraft,
$B(t)$ – the expected value of crack length for $m \neq 2$ which is determined by the following formula:

$$B(t) = [l_o^{\frac{2-m}{2}} + \frac{2-m}{2}\lambda C M_k^m\, \pi^{\frac{m}{2}}\, E[(\sigma^{\max})^m]t]^{\frac{2}{2-m}} - l_o \tag{10}$$

$A(t)$ – the variance of crack length for $m \neq 2$ which is determined by the following formula:

$$A(t) = \frac{2}{2+m} CM_k^m \pi^{\frac{m}{2}} \frac{E[(\sigma^{\max})^{2m}]}{E[(\sigma^{\max})^m]} \left[(l_o^{\frac{2-m}{2}} + \frac{2-m}{2} \lambda CM_k^m \pi^{\frac{m}{2}} E[(\sigma^{\max})^m]\, t)^{\frac{2+m}{2-m}} - l_o^{\frac{2+m}{2}} \right] \tag{11}$$

Notations:

M_k – coefficient of the finiteness of the element's dimensions and the location of crack;

$E[(\sigma^{\max})^{2m}] = P_1(\sigma_1^{\max})^{2m} + P_2(\sigma_2^{\max})^{2m} + ... + P_L(\sigma_L^{\max})^{2m}$;

$E[(\sigma^{\max})^m] = P_1(\sigma_1^{\max})^m + P_2(\sigma_2^{\max})^m + ... + P_L(\sigma_L^{\max})^m$;

l_0 – initial crack length;

λ – intensity of occurrence of loading cycles $(\lambda = \frac{1}{\Delta t})$;

Δt – duration time of loading cycle;

The density function of the flying time distribution up to the moment when crack value exceeds the limit value has the following form:

$$f(t)_{l_d} = \frac{\partial}{\partial t} Q(t; l_d) \tag{12}$$

The equation (12) can have the following form:

$$f_{l_d}(t) = \int_{l_d}^{\infty} \{ \frac{\partial}{\partial t} u(l,t) \}\, dl \tag{13}$$

Following the previous steps, if we want to determine the value of the integral (13), we must do the following:

- determine the derivative of time function $u(l, t)$, and
- find the integrand in the equation (13).

We determine the derivative of the time function (9) in the following way:

$$\frac{\partial}{\partial t}[u(l,t)] = \left(\frac{1}{\sqrt{2\pi\, A(t)}} \right)' e^{-\frac{(l-B(t))^2}{2A(t)}} + \left(\frac{1}{\sqrt{2\pi\, A(t)}} \right) \cdot \left(e^{-\frac{(l-B(t))^2}{2A(t)}} \right)' \tag{14}$$

Hence:

$$\frac{\partial}{\partial t}[u(l,t)] = -\frac{\lambda\hat{C}(l_o^{\frac{2-m}{2}} + \frac{2-m}{2}\hat{C}\lambda t)^{\frac{2m}{2-m}}}{2[(l_o^{\frac{2-m}{2}} + \frac{2-m}{2}\hat{C}\lambda t)^{\frac{2+m}{2-m}} - l_o^{\frac{2+m}{2}}](\frac{2}{2+m})}u(l,t) +$$

$$+\frac{(l_o^{\frac{2-m}{2}} + \frac{2-m}{2}\hat{C}\lambda t)^{\frac{m}{2-m}}\cdot(l-B(t))\,(\frac{2-m}{2})}{\frac{2}{2+m}\,\omega[(l_o^{\frac{2-m}{2}} + \frac{2-m}{2}\hat{C}\lambda t)^{\frac{2+m}{2-m}} - l_o^{\frac{2+m}{2}}]}u(l,t) +$$

$$+\frac{(l-B(t))^2\,\lambda(l_o^{\frac{2-m}{2}} + \frac{2-m}{2}\hat{C}\lambda t)^{\frac{2m}{2-m}}}{2\,\frac{4}{(2+m)^2}\,\omega[(l_o^{\frac{2-m}{2}} + \frac{2-m}{2}\hat{C}\lambda t)^{\frac{2+m}{2-m}} - l_o^{\frac{2+m}{2}}]^2}u(l,t) \qquad (15)$$

Now, we assume that the integrand in the equation (13) has the following form:

$$w(l,t) = u(l,t)\cdot\theta(l,t) \qquad (16)$$

where: $\theta(l,t)$ – the sought-after expression.

The derivative of the integrand $w(l,t)$ with respect to crack length shall be equal to expression (15). The derivative of the integrand with respect to l is

$$\frac{\partial w(l,t)}{\partial l} = u'(l,t)\,\theta(l,t) + u(l,t)\,\theta'(l,t) \qquad (17)$$

We determine the derivative:

$$\frac{\partial u(l,t)}{\partial l} = u(l,t)\left(-\frac{(l-B(t))}{A(t)}\right) \qquad (18)$$

Having considered (18), we obtain

$$\frac{\partial w(l,t)}{\partial l} = u(l,t)\left(-\frac{(l-B(t))}{A(t)}\right)\underbrace{(?)}_{\theta(l,t)} + u(l,t)\cdot\underbrace{(?)}_{\theta'(l,t)} \qquad (19)$$

We compare the equation (19) with (15):

$$\left\{ \frac{(l-B(t))(l_o^{\frac{2-m}{2}} + \frac{2-m}{2}\hat{C}\lambda t)^{\frac{m}{2-m}}(\frac{2-m}{2})\hat{C}}{\frac{2}{2+m}\omega\left[(l_o^{\frac{2-m}{2}} + \frac{2-m}{2}\hat{C}\lambda t)^{\frac{2+m}{2-m}} - l_o^{\frac{2+m}{2}}\right]\hat{C}} + \right.$$

$$+ \frac{(l-B(t))^2\lambda(l_o^{\frac{2-m}{2}} + \frac{2-m}{2}\hat{C}\lambda t)^{\frac{2m}{2-m}}\omega\hat{C}^2}{2\frac{4}{(2+m)^2}\omega\left[(l_o^{\frac{2-m}{2}} + \frac{2-m}{2}\hat{C}\lambda t)^{\frac{2+m}{2-m}} - l_o^{\frac{2+m}{2}}\right]^2\omega\hat{C}^2} -$$

$$\left. - \frac{\lambda\hat{C}(l_o^{\frac{2-m}{2}} + \frac{2-m}{2}\hat{C}\lambda t)^{\frac{2m}{2-m}}\hat{C}\omega}{2\left[(l_o^{\frac{2-m}{2}} + \frac{2-m}{2}\hat{C}\lambda t)^{\frac{2+m}{2-m}} - l_o^{\frac{2+m}{2}}\right]\hat{C}\omega(\frac{2}{2+m})} \right\} \tag{20}$$

$$u(l,t) = u(l,t)\underbrace{\left(-\frac{(l-B(t))}{A(t)}\right)(?)}_{\theta(l,t)} + u(l,t)\theta'(l,t)$$

We obtain the following solution of the equation (20):

$$u(l,t)\left\{ \frac{(l-B(t))(l_o^{\frac{2-m}{2}} + \frac{2-m}{2}\hat{C}\lambda t)^{\frac{m}{2-m}}(\frac{2-m}{2})\hat{C}}{\frac{2}{2+m}\omega\hat{C}\left[(l_o^{\frac{2-m}{2}} + \frac{2-m}{2}\hat{C}\lambda t)^{\frac{2+m}{2-m}} - l_o^{\frac{2+m}{2}}\right]} + \frac{(l-B(t))^2\lambda\omega\hat{C}^2(l_o^{\frac{2-m}{2}} + \frac{2-m}{2}\hat{C}\lambda t)^{\frac{2m}{2-m}}}{2\frac{4}{(2+m)^2}\omega^2\hat{C}^2\left[(l_o^{\frac{2-m}{2}} + \frac{2-m}{2}\hat{C}\lambda t)^{\frac{2+m}{2-m}} - l_o^{\frac{2+m}{2}}\right]^2} \right\} =$$

$$= u(l,t)\underbrace{\left(-\left(\frac{(l-B(t))}{A(t)}\right)\right)(?)}_{\theta(l,t)} \tag{21}$$

$$u(l,t)\left\{-\frac{\lambda\hat{C}^2\,\omega\,(l_o^{\frac{2-m}{2}}+\frac{2-m}{2}\,\hat{C}\lambda t)^{\frac{2m}{2-m}}}{2(\frac{2}{2+m})\hat{C}\omega\left[(l_o^{\frac{2-m}{2}}+\frac{2-m}{2}\,\hat{C}\lambda t)^{\frac{2+m}{2-m}}-l_o^{\frac{2+m}{2}}\right]}\right\}=u(l,t)\,\theta'(l,t) \quad (22)$$

We determine the function $\theta(l,t)$ from the equation (21):

$$\theta(l,t)=\left[\begin{array}{l}-(l_o^{\frac{2-m}{2}}+\frac{2-m}{2}\,\hat{C}\lambda t)^{\frac{m}{2-m}}(\frac{2-m}{2})\hat{C}\,\lambda- \\ -\frac{(l-B(t))\lambda\omega\hat{C}^2(l_o^{\frac{2-m}{2}}+\frac{2-m}{2}\,\hat{C}\lambda t)^{\frac{2m}{2-m}}}{2A(t)}\end{array}\right] \quad (23)$$

The derivative of the function determined by the equation (23) with respect to l is

$$\frac{\partial\theta(l,t)}{\partial l}=-\frac{\lambda\omega\hat{C}^2(l_o^{\frac{2-m}{2}}+\frac{2-m}{2}\,\hat{C}\lambda t)^{\frac{2m}{2-m}}}{2A(t)} \quad (24)$$

The obtained derivative confirms the rightness of the equation (22).

The abbreviated forms of quantities in the equations (21), (22), (23) and (24) mean the following:

$$B(t)=\left\{\left[(l_o^{\frac{2-m}{2}}+\frac{2-m}{2}\,\hat{C}\lambda t)^{\frac{2}{2-m}}-l_0\right]\right\} \quad (25)$$

$$A(t)=\frac{2}{2+m}\,\hat{C}\,\omega\left[(l_o^{\frac{2-m}{2}}+\frac{2-m}{2}\,\hat{C}\,\lambda t)^{\frac{2+m}{2-m}}-l_o^{\frac{2+m}{2}}\right] \quad (26)$$

$$\omega=\frac{E[(\sigma^{\max})^{2m}]}{(E[(\sigma^{\max})^m])^2} \quad (27)$$

$$\hat{C} = CM_k^m \pi^{\frac{m}{2}} E[(\sigma^{\max})^m] \tag{28}$$

Hence, we obtain the expression for the integrand of the integral (13):

$$w(l,t) = u(l,t)\left[\begin{array}{l} -(l_o^{\frac{2-m}{2}} + \frac{2-m}{2}\ \hat{C}\lambda t)^{\frac{m}{2-m}}(\frac{2-m}{2})\hat{C} - \\ -\frac{(l-B(t))\lambda\omega\hat{C}^2(l_o^{\frac{2-m}{2}} + \frac{2-m}{2}\ \hat{C}\lambda t)^{\frac{2m}{2-m}}}{2A(t)}) \end{array}\right] \tag{29}$$

Calculating the integral (13), we obtain the sought-after density function of the time (the flying time) of exceedance of the limit state.

$$f(t;l_d) = w(l,t)\Big|_{l_d}^{\infty} =$$

$$= u(l_d,t)\left[(l_o^{\frac{2-m}{2}} + \frac{2-m}{2}\ \hat{C}\lambda t)^{\frac{m}{2-m}}(\frac{2-m}{2})\ \hat{C}\lambda + \frac{(l_d - B(t))\lambda\omega\hat{C}^2(l_o^{\frac{2-m}{2}} + \frac{2-m}{2}\ \hat{C}\lambda t)^{\frac{2m}{2-m}}}{2(A(t))}\right] \tag{30}$$

where:
$$u(l_d,t) = \frac{1}{\sqrt{2\pi\ A(t)}} e^{-\frac{(l_d - B(t))^2}{2A(t)}} \tag{30a}$$

The equation (30) determines the density function of the fatigue limit of a selected element of aeronautical construction under conditions of the operating load spectrum for the Paris formula with the exponent $m \neq 2$.

3. The Outline of Estimation of Durability of Construction Element in an Aircraft with the Use of Distribution of Time of Exceedance of the Limit State for the Coefficient $m \neq 2$

The formula for the reliability of construction element with the use of the density function of time of the exceedance of the limit state can be written in the following form:

$$R(t) = 1 - \int_0^t f(t,l_d)\ dt \tag{31}$$

where the density function $f(t,l_d)$ is determined with formula (30).

Hence, the unreliability of construction element will be determined with the following formula

$$Q(t) = \int_0^t u(t, l_d)(B'(t) + \frac{(l_d - B(t))\, A'(t)}{2A(t)})\, dt \tag{32}$$

where:

$$B(t) = \left\{ \left[l_o^{\frac{2-m}{2}} + \frac{2-m}{2}\ \hat{C}\lambda t \right]^{\frac{2}{2-m}} - l_0 \right\}$$

$$A(t) = \frac{2}{2+m}\ \hat{C}\omega \left[\left(l_o^{\frac{2-m}{2}} + \frac{2-m}{2}\ \hat{C}\lambda t() \right)^{\frac{2+m}{2-m}} - l_0^{\frac{2+m}{2}} \right]$$

$u(t, l_d)$ – the function determined with the formula (30a).

Integral (32) shall be converted to a simpler form. Then, we must solve the indefinite integral

$$\int f(t, l_d)\, dt \tag{33}$$

We introduce the following change in the integrand

$$\underbrace{\frac{(l_d - B(t))^2}{2A(t)}}_{\text{"1"}} = \underbrace{\frac{(B(t) - l_d)^2}{2A(t)}}_{\text{"2"}} \tag{34}$$

We replace the expression 1 with the expression 2 and we mark the expression 2 with z.

Hence

$$\frac{(B(t) - l_d)^2}{2A(t)} = z \tag{35}$$

We calculate the derivative of equation (35) as follows:

$$\frac{dz}{dt} = \frac{2(B(t) - l_d)B'(t) \cdot 2A(t) - (B(t) - l_d)^2 (2A'(t))}{(2A(t))^2}$$

Hence

$$dt = \frac{(2A(t))^2}{2(B(t)-l_d)\,B^{'}(t)\cdot 2A(t)-(B(t)-l_d)^2(2A^{'}(t))}$$

We substitute into integral (33)

$$\int \frac{1}{\sqrt{2\pi A(t)}}\, e^{-z}\left(B^{'}(t)+\frac{(l_d-B(t)\,A^{'}(t)}{2A(t)}\right)\cdot\frac{(2A(t))^2}{2\{(B(t)-l_d)\,B^{'}(t)\cdot 2A(t)-(B(t)-l_d)^2A^{'}(t)\}}\,dz =$$

$$\frac{1}{2}\int \frac{1}{\sqrt{2\pi A(t)}}\, e^{-z}\left(\frac{2B^{'}(t)A(t)+(l_d-B(t))A^{'}(t)}{2A(t)}\right)\cdot\frac{(2A(t))^2}{\{(2B^{'}(t)A(t)-(B(t)-l_d)\,A^{'}(t)\}(B(t)-l_d)}\,dz =$$

$$= \frac{1}{2\sqrt{\pi}}\int \frac{1}{\sqrt{2A(t)}}\cdot\frac{(2A(t))}{(B(t)-l_d)}\,dz = \frac{1}{2\sqrt{\pi}}\int \frac{\sqrt{2A(t)}}{(B(t)-l_d)}\; e^{-z}\,dz$$

for

$$\frac{\sqrt{2A(t)}}{(B(t)-l_d)} = \frac{1}{\sqrt{z}}$$

Hence, after transformation we obtain the following:

$$\int t(t,l_d)\,dt = \frac{1}{2\sqrt{\pi}}\int \frac{1}{\sqrt{z}}\; e^{-z}\,dz \tag{36}$$

In integral (36), we shall perform the second substitution in the following form:

$$\sqrt{z} = w$$

$$\frac{dw}{dz} = \frac{1}{2\sqrt{z}}$$

$$\frac{dz}{dw} = 2w$$

Hence

$$dz = 2w\,dw \tag{37}$$

We substitute equation (37) into integral (36)

$$\frac{1}{2\sqrt{\pi}} \int \frac{1}{w} e^{-w^2} 2w \, dw = \frac{1}{\sqrt{\pi}} \int e^{-w^2} \, dw \tag{38}$$

We perform one more substitution

$$w^2 = \frac{y^2}{2}$$

$$2w \, d \, w = y \, d \, y$$

$$dw = \frac{y}{2w} dy$$

$$dw = \frac{dy}{\sqrt{2}} \tag{39}$$

Hence, after substitution (39) into (38) we obtain the integral

$$\frac{1}{\sqrt{2\pi}} \int e^{-\frac{y^2}{2}} \, dy$$

where y adopts the value which is determined by the equation (40), because:

$$\frac{y^2}{2} = w^2; \qquad w = \sqrt{z}; \qquad z = \frac{(B(t) - l_d)^2}{2 A(t)}$$

$$w = \sqrt{\frac{(B(t) - l_d)^2}{2 A(t)}}$$

$$w = \frac{(B(t) - l_d)}{\sqrt{2 A(t)}}$$

The last substitution:

$$w^2 = \frac{y^2}{2}$$

$$y^2 = 2w^2$$

$$y = w\sqrt{2} = \sqrt{2} \cdot \frac{(B(t) - l_d)}{\sqrt{2 A(t)}} \tag{40}$$

After substituting the obtained results into formula (31) and remembering about the proper notation of integration limits we obtain the following formula for the reliability.

$$R(t) = 1 - \frac{1}{\sqrt{2\pi}} \int_{-\infty}^{y(t)} e^{-\frac{y^2}{2}} dy \tag{41}$$

Hence, the unreliability of aircraft construction element will be determined with the following equation

$$Q(t) = \frac{1}{\sqrt{2\pi}} \int_{-\infty}^{\frac{(B(t)-l_d)}{\sqrt{A(t)}}} e^{-\frac{y^2}{2}} dy \tag{42}$$

Assuming the risk level of construction element damage, i.e. the level of exceedance of a current value of crack length, we obtain the following value

$$Q(t) = Q^* \tag{43}$$

Hence

$$Q^* = \frac{1}{\sqrt{2\pi}} \int_{-\infty}^{\theta} e^{-\frac{y^2}{2}} dy \tag{44}$$

Having the value Q^*, we read the value of the upper limit of integral (44) from the Table of the Standard Normal Distribution. Thus, we obtain the value θ.

Hence, we obtain the equation for independence of determination of element durability for the assumed level of risk.

$$\theta = \frac{(B(t) - l_d)}{\sqrt{A(t)}} \tag{45}$$

In equation (45) we look for such value t^* that in equation (45) the left side of the equation equals to the right one. Thus, by solving equation (45) we determine the sought-after durability of aircraft construction element.

4. Final Remarks

Both this article and the second one that was published in the form of a report at KONES conference, [3] present the probabilistic method for estimation of the fatigue limit in construction elements comprehensively with the use of the Paris formula.

The article [3] concerns the case when the material constant in the Paris formula is equal to $m = 2$.

This article concerns the case when the material constant in the Paris formula is $m \neq 2$

In this method, the factor causing fatigue is the random loading in the form of the loading spectrum. This method requires numerical verification in respect of appropriately prepared data.

The obtained equations enable precise calculations when we have the values of material constants and data concerning the loading spectrum.

It shall be mentioned that it is possible to determine the fatigue limit of construction element in case of more complicated loading spectrum.

References

[1] Smirnov N.N, Ickowicz A.A.; „Obstuzivanije i remont aviucjonnej techniki po sostojaniju". Transport, 1980.
[2] Kałmucki W.S.; „Prognozirowanije resursov detali maszin i elementow konstrukcji". Kisziniev, 1989.
[3] Tomaszek H., Klimaszewski S., Zieja M.; „Zarys probabilistycznej metody wyznaczania trwałości zmęczeniowej elementu konstrukcji z wykorzystaniem wzoru Parisa i funkcji gęstości czasu przekraczania stanu granicznego".
[4] Tomaszek H., Żurek J., Jasztal M.; „Prognozowanie uszkodzeń zagrażających bezpieczeństwu lotów statków powietrznych". Wydawnictwo Naukowe JTE – PIB, Radom, 2008.
[5] Tomaszek H., Ważny M.; „Zarys metody oceny trwałości na zużycie powierzchniowe elementów konstrukcji z wykorzystaniem rozkładu czasu przekraczania stanu granicznego". ZEM, 2008.

Manuscript received by Editorial Board, January 15th, 2010

Zarys metody wyznaczenia trwałości zmęczeniowej elementu konstrukcji lotniczej z wykorzystaniem funkcji gęstości czasu przekraczania stanu granicznego

S t r e s z c z e n i e

W pracy [3] przedstawiono zarys probabilistycznej metody wyznaczania trwałości zmęczeniowej elementu konstrukcji z wykorzystaniem wzoru Parisa dla $m = 2$ i funkcji gęstości czasu przekraczania stanu granicznego (dopuszczalnego). W niniejszym artykule przedstawiona została również metoda wyznaczania trwałości zmęczeniowej elementu konstrukcji dla funkcji gęstości czasu przekraczania stanu granicznego (dopuszczalnego) i wzoru Parisa dla $m \neq 2$.

Do modelowania pękania zmęczeniowego w ujęciu losowym wykorzystano równania różnicowe oraz równanie Fokkera-Plancka. Rozwiązanie równania Fokkera-Plancka jest poszukiwaną funkcją gęstości długości pęknięcia elementu, którą następnie wykorzystano do znalezienia funkcji gęstości czasu przekraczania stanu dopuszczalnego pęknięcia.

Ta ostatnia funkcja gęstości posłużyła do oszacowania trwałości zmęczeniowej.

SCIENTIFIC PROBLEMS
OF MACHINES OPERATION
AND MAINTENANCE
3 (159) 2009

ZBIGNIEW KŁOS*

First research works on LCA at Poznań University of Technology

Key words

LCA, first research, Poznań University of Technology.

Słowa kluczowe

LCA, pierwsze badania naukowe, Politechnika Poznańska.

Summary

In this paper the early works done in the field of Life Cycle Assessment (LCA) at Poznań University of Technology (PUT) are presented. The first part of the paper is focused on the methodology of LCA. Then one of the first research works on LCA in Poland, performed at Poznań University of Technology, is presented. It is the environmental valuation of three packaging machines. Their technical data and general aim of research are shown as well as the elementary goals: the description and comparison of environmental interactions of packaging machines, the identification of the areas of the significant environmental impacts, finding the possible improvement opportunities in the life cycle, and an indication of the directions for whole system of machines' optimisation. The way to achieve these goals is presented in the paper.

* Poznań University of Technology, Faculty of Working Machines and Transportation, Institute of Working Machines and Motor Vehicles, Piotrowo 3 St., 60-965 Poznań, Poland.

1. About life cycle assessment

1.1. What is LCA?

Turning the consumer society in a more sustainable direction seems to be hard to do. Therefore, the tool – life cycle assessment (LCA) was developed. It is the method that makes easier analysis of the environmental impact of products, i.e. goods and services. The idea of LCA was developed in the second part of XX century. Generally, the concept of life cycle is defined as a process in which the inputs to the "cycle" and outputs from the "cycle" are evaluated for each step of the object of analysis. The cycle begins at the concept of the object and completes with the recycle or disposal phase [1]. The idea of life cycle is especially useful when considering the object development.

The LCA of the object

- is defined as a process aimed at identifying the negative effects of this object,
- quantifies the use of raw materials, energy consumption and emissions,
- evaluates the impact of these uses made of energy and materials as well as emissions into the environment, and
- evaluates the relevant improvements in an environmental context.

The standard ISO 14040 describes LCA as a technique for assessing the environmental aspects and potential impacts associated with a product, by [2]

- compiling an inventory of relevant inputs and outputs of a product system,
- evaluating the potential environmental impacts associated with those inputs and outputs, and
- interpreting the results of the inventory analysis and impact assessment phases in relation to the objectives of the study.

1.2. How is LCA structured?

The LCA methodology is composed of several interrelated elements:

1) goal and scope definition,
2) inventory analysis,
3) impact assessment,
4) interpretation (Fig. 1).

The goal and scope definition is an integral part in the LCA procedure. This step is required at an early stage in the study to gain a clear understanding of the purpose, to specify the system to be studied, and to determine the relevant requirements for peer review and communication of results.

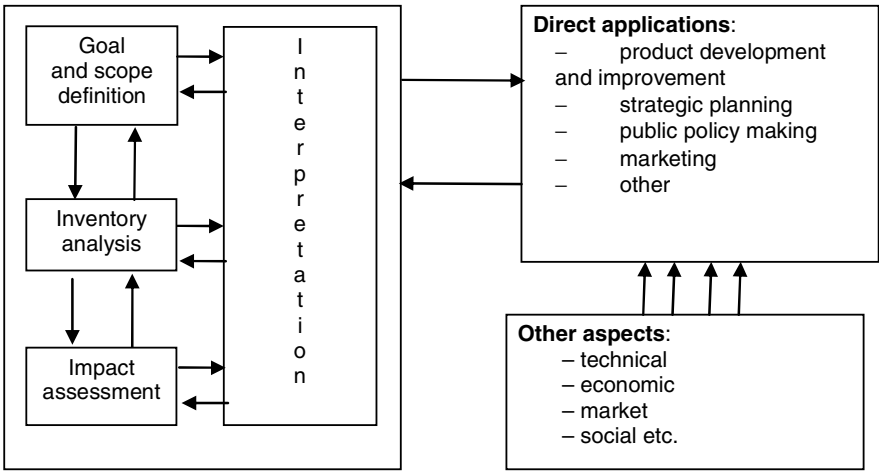

Fig. 1. Structure of LCA [3]
Rys. 1. Struktura LCA [3]

2. Example of one of the first Poznan University of Technology Works on LCA

Investigation on environmental valuation of packaging machines: PCGb01, PCGf02 and PCGi01 was one of the first research works on LCA, performed at Poznań University of Technology. Their technical data are presented below (Tab. 1).

Table 1. Technical data of analysed machines
Tabela 1. Techniczne dane badanych maszyn

Technical data	Unit	Packaging machine		
		PCGb01	PCGf02	PCGi01
Output	bot/h	2300	4500	7000
Consumption power	kW	2.2	2.2	4.8
Quantity of pourers	pieces	20	36	40
Quantity of closing heads	pieces	6	8	8
Pressure of packed fluid	MPa	0.6	0.6	0.8
Pressure of air	MPa	0.5	0.5	0.5
Air consumption	m^3/h	4	5	8
CO_2 consumption*	m^3/h	2.8	5.0	7.0
Noise level	dB	85	85	85
Overall dimensions (height × length × width)	mm	2490 × 2080 × 1450	2530 × 2895 × 2125	2860 × 2982 × 2610
Mass	kg	2600	5100	6080
* used in the filling process				

A general aim of this LCA study was the complex environmental evaluation of selected types of packaging machines. As elementary goals there were as follows:

1) A description and comparison of environmental interactions of packaging machines,
2) The identification of the areas of the significant environmental impacts (so called hot spots),
3) Finding the possible improvement opportunities in the life cycle, and
4) An indication of the directions for whole system of machines optimisation.

Data collection processes focused on the following:

- material production processes,
- energy, transport, and wastes,
- composite materials.

The functional unit was the environmental cost of filling 1000 litre beverage into the bottles.

Materials used for the production of the chosen packaging machines and during the operation period, with reference to the functional unit, are presented respectively in Tab. 2 and Tab. 3. Further, the media used in the whole life of packaging machines are presented (Tab. 4).

Table 2. Materials used for the production of chosen packaging machines, with reference to functional unit (part) [g]
Tabela 2. Materiały użyte do produkcji badanych maszyn pakujących w odniesieniu do jednostki funkcjonalnej (zestawienie ważniejszych pozycji) [g]

Material	Packaging machines		
	PCGb01	PCGf02	PCGi01
Bars	0.013913	0.013333	0.008096
Sheets	0.752187	1.373752	0.935673
bars	2.482361	2.170449	1.132205
sheets	5.154387	4.389882	4.522311
forgings	1.79433	1.736102	0.724694
bars	0.87731	1.065077	0.519906
sheets	0.898566	0.868347	0.367665
The others	0.929001	0.654581	0.435134
bars	0.005217	0	0.00127
others	0.001256	0.001284	0.000953
bars	1.016153	0.429408	0.507683
sheets	1.292293	0.741391	0.363061
forgings	0	0	0.07239
others	0.637789	0.35998	0.218123

Table 3. Materials used in the operation period of chosen packaging machines, with reference to functional unit (part) [g]
Tabela 3. Materiały użyte w eksploatacji maszyn pakujących w odniesieniu do jednostki funkcjonalnej (zestawienie ważniejszych pozycji) [g]

Material	Packaging machines		
	PCGb01	PCGf02	PCGi01
St3SX	1.410652	0.362449	0.313055
St5	1.8763604	1.170306	0.646113
45	2.5237144	1.550532	1.088708
0H17T	0.2724684	0.040492	0.02413
1H18N9T	0.1565244	0.052837	0.058103
3H13	0.0975862	0.004444	0.01016
Zs60003	0	0.301218	0.136843
B555	0.067634	0	0.02921
BA1032	0.1053158	0	0.010795
MO59	0.0028986	0	0
Hydraulic oil	0.521748	0.335784	0.2921
Transol oil	4.3479	2.91342	0.6985
Compressor's oil	0.927552	0.632064	0.5207
ŁT43 grease	0.77296	0.553056	0.2159
Aliten grease	0.0222226	0.012345	0.00889
Defenzor grease	0.0502424	0.036047	0.025718

Table 4. Utility used in the whole life cycle of packaging machines with reference to the functional unit
Tabela 4. Media użyte w całym cyklu życia maszyn pakujących w odniesieniu do jednostki funkcjonalnej

Medium	Packaging machines		
	PCGb01	PCGf02	PCGi01
Sterile air [m^3]	1.15944	0.7407	0.762
CO_2 [m^3]	0.811608	0.7407	0.66675
Electric energy [kWh]:			
- to production	0.162747	0.084815	0.11639
- to operating	0.63769	0.32591	0.4572

An impact assessment was carried out with the support of SimaPro 4.0 programme, using Ecoindicator 95 procedure.

Subdivision of environmental impact was into ten categories:

1) greenhouse effect,
2) ozone layer depletion,
3) acidification,
4) eutrophication,
5) heavy metals emission,
6) carcinogenicity,
7) winter smog,
8) summer smog,
9) energy depletion,
10) solid emissions.

Calculations were carried out with respect to the division of the whole life cycle into

- production (with further division into metallic and other materials),
- operating period (with further division into materials and media),
- distribution, and
- final disposal.

The results of the characterisation phase and the normalisation phase for analysed machines, with reference to the functional unit, are presented, respectively, in Tab. 5 and Tab. 6.

Table 5. Results of the characterisation phase of packaging machines with reference to the functional unit
Tabela 5. Rezultaty fazy charakteryzowania maszyn pakujących w odniesieniu do jednostki funkcjonalnej

Impact category	Unit	Packaging machine		
		PCGb01	PCGf02	PCGi01
greenhouse effect	kg CO_2	1.17	0.617	0.827
Ozone layer depletion	kg CFC11	4.78E-8	9.08E-9	8.16
acidification	kg SO_2	0.0098	0.00618	0.00725
eutrophication	kg PO_4	0.000278	0.000151	0.000183
Heavy metals emission	kg Pb	1.4E-6	6.49E-7	8.5E-7
carcinogenicity	kg B(a)P	2.16E-8	1.37E-8	1.37E-8
winter smog	kg SPM*	0.00823	0.00534	0.00621
summer smog	kg C_2H_4	7.12E-5	-0.000133	-0.000103
energy depletion	MJ	14.3	5.76	7.55
solid emissions	kg	0.273	0.228	0.209
* SPM = Suspended Particulate Matter				

Table 6. Results of the normalisation phase of packaging machines with reference to the functional unit
Tabela 6. Rezultaty fazy normalizacji maszyn pakujących w odniesieniu do jednostki funkcjonalnej

Impact category	Packaging machine		
	PCGb01	PCGf02	PCGi01
greenhouse effect	8.99E-5	4.72E-5	6.33E-5
ozone layer depletion	5.17E-8	9.81E-9	8.82E-9
acidification	8.7E-5	5.49E-5	6.44E-5
eutrophication	7.27E-6	3.96E-6	4.8E-6
heavy metals emission	2.57E-5	1.19E-5	1.56E-5
carcinogenicity	1.99E-6	1.26E-6	1.26E-6
winter smog	8.27E-5	5.67E-5	6.58E-5
summer smog	3.98E-6	-7.43E-6	-5.77E-6
energy depletion	8.97E-5	3.62E-5	4.75E-5
solid emissions	0	0	0

The results of the environmental analyse of chosen objects show that the most environmentally friendly machine is the PCGf02. The environmental burden caused by PCGb01 is about 70% and by PCGi01 is about 20% greater than in the case of PCGf02 (Fig. 2).

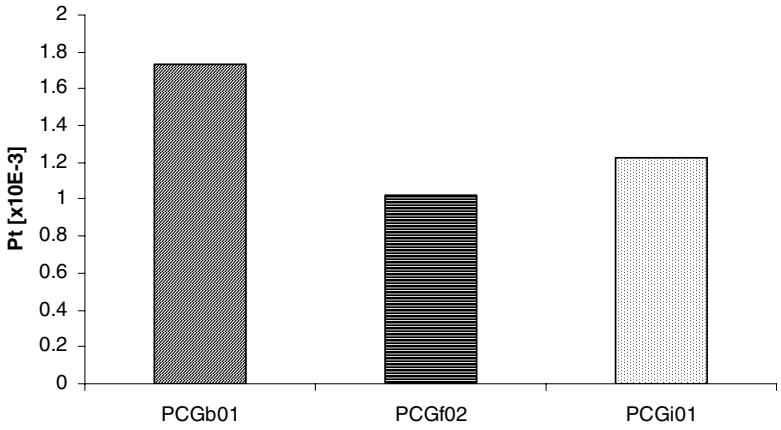

Fig. 2. Comparison of environmental indexes of packaging machines
Rys. 2. Porównanie wskaźników środowiskowych badanych maszyn pakujących

Dominating interactions result in such consequences as acidification, winter smog, and the greenhouse effect (Fig. 3).

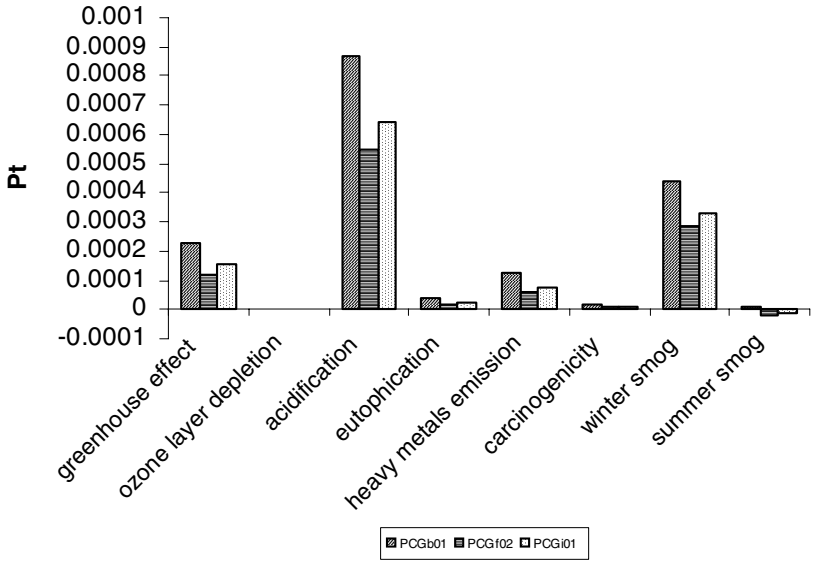

Fig. 3. Environmental profile of packaging machines
Rys. 3. Środowiskowy profil badanych maszyn pakujących

Review of environmental impacts with reference to the division into the main stages of packaging machines life cycle shows that the dominating environmental burdens are associated with operating period. Positive environmental impacts of the disposal stage of packaging machines (about 5.5% of all impacts) diminish the consequences of the rest of harmful interactions (Fig. 4).

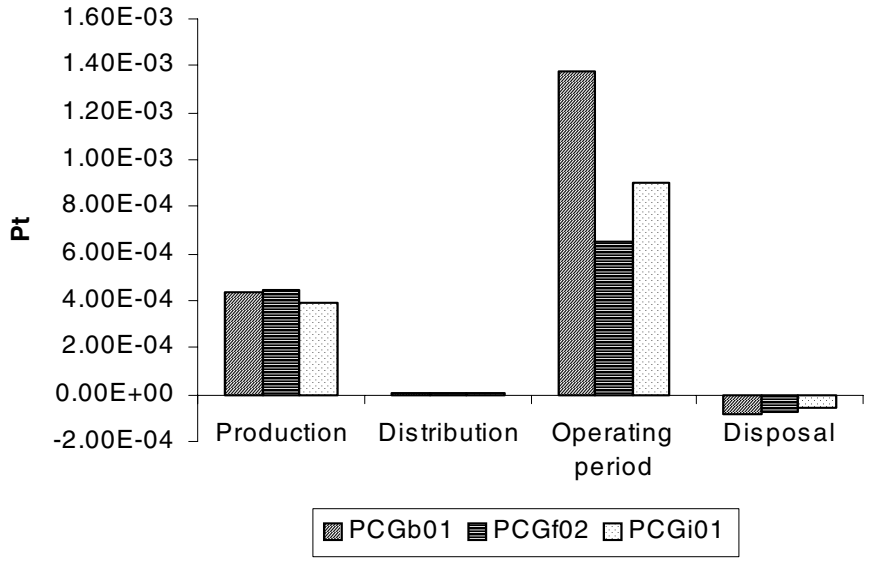

Fig. 4. Environmental indexes connected with stages of packaging machines' life cycle
Rys. 4. Wskaźniki środowiskowe dla etapów życia badanych maszyn pakujących

3. Hints for designers of technical objects

Described above is the first research on LCA in Poznań University of Technology, and it allows one to draw the following conclusions:

1) Designers have to be able to assess the following:
   - priorities, (They have to know where the biggest gains can be made.) and
   - which design solution is better from the environmental point of view.
2) Very often it is possible to reduce the amount of materials by critically looking at dimensions, required strength and production techniques.
3) Product design should aim at
   - reducing total material content,
   - minimising the total number of different materials,
   - preferring materials which can be recycled, and/or use biodegradable,
   - find materials to replace non-biodegradable materials,
   - minimising the use of energy-intensive materials,
   - minimising energy consumed in use, and
   - going for the form of energy with the lowest contribution to greenhouse gases production where there is a choice of energy supply.
4) Actually, designers must understand the relationship between a product and the environment before a product can be developed in a truly environmentally sound way.

From above conclusions, the following suggestions arise:

1) To meet above mentioned requirements, it is worth using LCA methodology, which can determine indicators (environmental indices, indexes) of existing different materials. Environmental indicators (indexes) concern the following groups:
   a) construction materials for machines and vehicles: steel (construction, high quality, automatic, stainless etc.), cast iron, plastic, glass, rubber, etc.,
   b) technological processes (for different materials): casting, welding, forging, etc.,
   c) electric energy production in:
      – coal power plant,
      – lignite power plant,
      – oil or gas power plant,
      – nuclear power plant,
      – hydro power plant,
   d) transportation processes, on road, water, and in air,
2) The received environmental indexes are presented in useful units, in case of
   – materials - by 1 kg of materials,
   – energy - by 1 kWh of produced energy,
   – technology - by 1 kg cast or forging, by 1 m welding joint, by 1 m2 of surface, and
   – transport - by 1 km of transported substances.

As an example, the environmental indexes for different technological processes (Tab. 7) and different means of transportation (Tab. 8) are presented below.

Table 7. Environmental indexes for different technological processes
Tabela 7. Wskaźniki środowiskowe dla różnych procesów technologicznych

Technological process	Environmental index [Pt]	Unit
Casting	0.00657	1 kg of casting materials
Forging	5.9E-04	1 kg of forging materials
Drawing	1.6E-05	1 kg of drawing materials
	2.7E-04	1 kg of plastic
plastic forming	0.0334	1 m of welding
welding	4.2E-04	1 m of welding
laser cutting	2.2E-04	1 kg of machining
machining	3.3E-04	1 kg of injection moulding
injection moulding	0.00899	1 m of welding
	2.3E-04	1 kg of machined material
MIG welding		
turning		

Table 8. Environmental indexes for different means of transportation
Tabela 8. Wskaźniki środowiskowe dla różnych środków transportu

Transportation means	Environmental index 1 tkm [Pt]
truck 28t	1.4E-04
truck 16t	3.4E-04
truck (in a city transport)	4.8E-04
railway (electric)	1.06E-04
railway (IC engine)	1.32E-04
barge	5.5E-05
container ship	5.6E-05
coaster	2.0E-05
bulk carrier	3.4E-05
tanker	9.7E-05

4. Conclusions

Following conclusions can be drawn from this paper:

1) The first research works were done based on available tools – SimaPro 4.0 and Ecoindicator 95. The results showed the usefulness of the tools and procedure applied to evaluate analysed objects.
2) Research results give a clear indication about which object is the most environment friendly one: PCGf02.
3) It was confirmed that, in the case when an object works for a long time, (10 or more years) the operation period creates dominating environmental burdens.
4) The selection of construction materials concerning the environment should be based on two main criteria:
   – The influence of materials on the environment, defined by environmental indexes for materials and raw materials, and
   – The influences of technological processes on the environment, defined by environmental indexes for these processes.
5) The presented example also shows the directions of LCA research started at PUT: first, the environmental analyses of technical objects, then, the creation of the databases concerning materials and different technology.

References

[1] Life Cycle Assessment. A Guide to Approaches, Experiences and Information Sources. European Environmental Agency, Copenhagen 1998.

[2] PN-EN ISO 14040:2000, Zarządzanie Środowiskowe – Ocena cyklu życia – Zasady i struktura.

[3] Kłos Z., Kurczewski P., Kasprzak J., Środowiskowe charakteryzowanie maszyn i urządzeń. Podstawy ekologiczne, metody i przykłady. Poznań, Wydawnictwo Politechniki Poznańskiej 2005.

Manuscript received by Editorial Board, December 01st, 2008

Pierwsze badania nad LCA w Politechnice Poznańskiej

S t r e s z c z e n i e

W artykule dokonano prezentacji pierwszych badań w obszarze LCA, prowadzonych w Politechnice Poznańskiej. Pierwsza część artykułu jest zorientowana na metodologię LCA. Potem są zaprezentowane jedne z pierwszych badań nad LCA w Polsce, wykonane w Politechnice Poznańskiej. Jest to oceną środowiskowa trzech maszyn pakujących. Przedstawione są ich dane techniczne. Wskazane są cele szczegółowe badań: opis i porównanie oddziaływania środowiskowego tych maszyn, identyfikacja oddziaływań o szczególnym znaczeniu, znalezienie okazji do zmniejszenia oddziaływania badanych maszyn w cyklu życia i kierunków optymalizacji całego systemu tych maszyn. Droga do osiągnięcia tych celów jest przedstawiona w artykule.